Accepted Manuscript

Vibrational spectroscopic and molecular docking study of (2*E*)-*N*-(4-chloro-2-oxo-1,2-dihydroquinolin-3-yl)-3-phenylprop-2-enamide

Rajeev T. Ulahannan, C. Yohannan Panicker, Hema Tresa Varghese, Robert Musiol, Josef Jampilek, Christian Van Alsenoy, Javeed Ahmad War, Abdulaziz A. Al-Saadi

PII: S1386-1425(15)30013-5
DOI: http://dx.doi.org/10.1016/j.saa.2015.06.083
Reference: SAA 13853

To appear in: *Spectrochimica Acta Part A: Molecular and Biomolecular Spectroscopy*

Received Date: 10 November 2014
Revised Date: 20 June 2015
Accepted Date: 22 June 2015

Please cite this article as: R.T. Ulahannan, C. Yohannan Panicker, H.T. Varghese, R. Musiol, J. Jampilek, C.V. Alsenoy, J.A. War, A.A. Al-Saadi, Vibrational spectroscopic and molecular docking study of (2*E*)-*N*-(4-chloro-2-oxo-1,2-dihydroquinolin-3-yl)-3-phenylprop-2-enamide, *Spectrochimica Acta Part A: Molecular and Biomolecular Spectroscopy* (2015), doi: http://dx.doi.org/10.1016/j.saa.2015.06.083

Vibrational spectroscopic and molecular docking study of (2*E*)-*N*-(4-chloro-2-oxo-1,2-dihydroquinolin-3-yl)-3-phenylprop-2-enamide

Rajeev T.Ulahannan[a], C.Yohannan Panicker[a]*, Hema Tresa Varghese[b], Robert Musiol[c], Josef Jampilek[d], Christian Van Alsenoy[e], Javeed Ahmad War[f], Abdulaziz A.Al-Saadi[g]

[a]Department of Physics, TKM College of Arts and Science, Kollam, Kerala, India

[b]Department of Physics, Fatima Mata National College, Kollam, Kerala, India

[c]Institute of Chemistry, University of Silesia, Szkolna 9, 40007 Katowice, Poland.

[d]Department of Chemical Drugs, Faculty of Pharmacy, University of Veterinary and Pharmaceutical Sciences Brno, Palackeho 1/3, 61242 Brno, Czech Republic

[e]University of Antwerp, Chemistry Department, Universiteitsplein 1, B2610 Antwerp, Belgium.

[f]Department of Chemistry, Dr.H.S.Gour Central University, Sagar, M.P. 470003, India

[g]Department of Chemistry, King Fahd University for Petroleum and Minerals, Dhahran 31261, Saudi Arabia

*author for correspondence: email: cyphyp@rediffmail.com

Phone: 91 9895370968

Abstract

FT-IR and FT-Raman spectra of (2*E*)-*N*-(4-chloro-2-oxo-1,2-dihydroquinolin-3-yl)-3-phenylprop-2-enamide were recorded and analyzed experimentally and theoretically. The synthesis, ^{1}H-NMR and PES scan results are also discussed. Nonlinear optical behaviour of the examined molecule was investigated by the determination of first hyperpolarizability. The calculated HOMO and LUMO energies show the chemical activity of the molecule. The stability of the molecule arising from hyper-conjugative interaction and charge delocalization has been analyzed using NBO analysis. From the MEP it is evident that the negative charge covers the carbonyl group and the positive region is over the NH group. The calculated geometrical parameters (SDD) are in agreement with that of similar derivatives. Molecular docking simulations against targets from *mycobacterium tuberculosis* are reported and the results suggest that the compound might exhibit inhibitory activity against PknB.

Keywords: DFT; FT-IR; FT-Raman; quinoline; MEP; Molecular docking.

1. Introduction

Quinoline derivatives have been extensively studied due to their anti-amoebic [1], anti-viral [2], anti-parasitic [3], anti-malarial [4-10] properties. Quinolines have good electron mobility, good thermal and oxidative stabilities, high photoluminescence efficiencies and

good film forming properties which is important for their use in organic light emitting diodes (OLEDs) [11, 12]. Quinolines are reported to be a promising candidate for the use as PhOLEDs (Phosphorescent Organic Light Emitting diodes) [13] with good nonlinear optical properties [14, 15]. There has been growing interest in using organic materials for nonlinear optical devices, functioning as second harmonic generators, frequency converters, electro-optical modulators, etc. because of the large second order electric susceptibilities of organic materials. Since the second order electric susceptibility is related to first hyperpolarizability, the search for organic chromophores with large first hyperpolarizability is fully justified. The organic compounds showing high hyperpolarizability are those containing an electron donating group or an electron withdrawing group interacting through a system of conjugated double bonds. To the best of our knowledge, a detailed description of the spectroscopic behaviour of the title compound with the help of vibrational spectral techniques and quantum chemical calculations along with NLO properties has not been given to date. Due to the different potential biological activity of the title compound, molecular docking of the title compound is also reported.

2. Experimental details

General procedure for the preparation of (2*E*)-*N*-(4-chloro-2-oxo-1,2-dihydroquinolin-3-yl)-3-phenylprop-2-enamide

All reagents were purchased from Aldrich. TLC experiments were performed on alumina-backed silica gel 40 F254 plates (Merck, Darmstadt, Germany). The plates were illuminated under UV (254 nm) and evaluated in iodine vapour. The melting points were determined on BoetiusPHMK 05 (VEBKombinatNagema, Radebeul, Germany) and are uncorrected. Elemental analyses were carried out on an automatic Perkin-Elmer 240 microanalyser (Boston, USA). ^{1}H-NMR spectrum was recorded on a Bruker AM-500 (500 MHz for ^{1}H), Bruker BioSpin Corp., Germany. Chemicals shifts are reported in ppm (δ) to internal $Si(CH_3)_4$, when diffused easily exchangeable signals are omitted. Mass spectra were measured using a LTQ Orbitrap Hybrid Mass Spectrometer (Thermo Electron Corporation, USA) with direct injection into an APCI source (400 °C) in the positive mode.

Aniline (5mmol) and malonic acid (5mmol) were thoroughly mixed with 20g PPA and heated under stirring in microwave reactor at 400W during 2×20 minutes with 5 minutes interval. The temperature reached 210°C. Then the mixture was poured into crushed ice and the beige solid was filtered and purified by extraction with EtOH and a white crystalline compound 4-hydroxyquinolin-2(1*H*)-one was obtained in yield 35% [16]. 4-Hydroxy-3-

nitroquinolin-2(1*H*)-one was obtained according to the described nitration procedure [17] as a yellow crystalline compound in yield 71%. Nitro derivative (9.7mmol) and tin powder (32mmol) were stirred with 36% HCl (8.1mL). The mixture was warmed at 80-90°C for 30 min. The brown solution was cooled to room temperature and filtered. The filtrate was alkalized with NH_3(aq) and warmed for 20 min. Then Celite was added and filtered. The solid was washed thoroughly with hot water (80°C). The combined filtrates were concentrated and acidified. After cooling 3-amino-4-hydroxyquinolin-2(1*H*)-one as a white crystalline compound was obtained in yield 85% [16]. 3-Amino-4-chloroquinolin-2(1*H*)-one was obtained according to the described chloration procedure with $POCl_3$, Et_3N under reflux 30 min in acetonitrile [17]. This compound (1mmol) was mixed with water (5mL), Et_2O (5mL) and sodium bicarbonate (0.3g). The resulted mixture was stirred in an ice bath (-3°C) and 10mL of Et_2O solution of cinamoyl chloride (1mmol) was added slowly. The resulting mixture was stirred at ambient temperature for 2 days, cooled in fridge and filtered. Et_2O was added to the solid and dried. A white crystalline compound was obtained (supporting information: Scheme.1).

The FT-IR spectrum (Fig. 1) was recorded using KBr pellets on a DR/Jasco FT-IR 6300 spectrometer. The spectral resolution was 4 cm^{-1}. The FT-Raman spectrum (Fig. 2) was obtained on a Bruker RFS 100/s, Germany. For excitation of the spectrum the emission of Nd:YAG laser was used with excitation wavelength 1064 nm and maximal power 150mW; measurement were performed on solid samples. One thousand scans were accumulated with a total registration time of about 30 min. The spectral resolution after apodization was 2 cm^{-1}.

3. Computational details

Calculations of the title compound are carried out with Gaussian09 program [18] using the HF/6-31G (6D, 7F), B3LYP/6-31G (6D, 7F) and B3LYP/SDD quantum chemical calculation methods to predict the molecular structure and vibrational wave numbers. Molecular geometry was fully optimized by Berny's optimization algorithm using redundant internal coordinates. Harmonic vibrational wave numbers are calculated using the analytic second derivatives to confirm the convergence to minima on the potential surface. The wave number values computed at the Hartree-Fock level contain known systematic errors due to the negligence of electron correlation. We therefore, have used the scaling factor value of 0.8929 for HF method. The DFT hybrid B3LYP functional and SDD methods tend to overestimate the fundamental modes, therefore scaling factor of 0.9613 has to be used for obtaining a considerably better agreement with experimental data [19]. The Stuttgart/Dresden

effective core potential basis set (SDD) was chosen particularly because of its advantage of doing faster calculations with relatively better accuracy and structures [20, 21]. Then frequency calculations were employed to confirm the structure as minimum points in energy. Parameters corresponding to optimized geometry (SDD) of the title compound (Fig. 3) are given in Table 1. The absence of imaginary wavenumbers on the calculated vibrational spectrum confirms that the structure deduced corresponds to minimum energy. The assignments of the calculated wave numbers are aided by the animation option of GAUSSVIEW program, which gives a visual presentation of the vibrational modes [22]. The potential energy distribution (PED) is calculated with the help of GAR2PED software package [23].

4. Results and discussion

4.1 IR and Raman spectra

The observed IR and Raman bands, calculated (scaled) wavenumbers and assignments are given in Table 2. The N-H stretching vibrations give rise to bands at 3500-3300 cm^{-1} [24, 25]. According to Roeges the N-H stretching vibration appears strongly and broadly in the region 3390 ± 60 cm^{-1} [26]. For the title compound N-H stretching modes are assigned at 3419 and 3467 cm^{-1} theoretically (SDD) and a strong band is observed in the IR spectrum at 3377 cm^{-1}. Mary et al. [27] reported a band at 3343 cm^{-1} in the IR spectrum, 3340 cm^{-1} in Raman spectrum and 3433 cm^{-1} theoretically as N-H stretching mode. The C-N-H vibration in which N and H atoms move in opposite direction of carbon atom in the amide moiety is reported at 1497 cm^{-1} theoretically, and the C-N-H vibration in which N and H atoms move in the same direction of carbon atom in the amide group is reported at 1217 cm^{-1} (DFT) [28-30]. For the title compound the bands at 1490 (IR) and 1474, 1235 cm^{-1} (SDD) is assigned as N-H in-plane bending mode. The out-of-plane bending of NH is expected around 650 ± 50 cm^{-1} [26]. In the present case the band at 675 (IR), 666 (Raman) and 668 cm^{-1} (SDD) is assigned as out-of-plane bending of N-H. According to literature, if N-H is a part of a closed ring the C-N-H deformation band is absent in the region 1510-1500 cm^{-1} [26, 31]. For the title compound the N_{11}-H_{12} deformation band is observed at 1383 cm^{-1} theoretically. The out-of-plane N-H deformation is theoretically assigned at 728 cm^{-1} for N-H being a part of the ring. Minitha et al. [32] reported δNH at 1300 cm^{-1} and γNH at 535 cm^{-1}. The C_{17}-N_{18} stretching is assigned at 1196 cm^{-1} (IR), 1199 cm^{-1} (Raman) and 1187 cm^{-1} theoretically. Louran et al. [33] reported a value at 1220 cm^{-1} for υC-N for poly aniline. In the case of aromatic amines a strong C-N stretching absorption is observed in the region in 1342-1266

cm^{-1} [28, 34]. Varghese et al. [35] reported υC-N mode at 1203 cm^{-1} in the IR spectrum and at 1208 cm^{-1} theoretically.

The band observed at 1595 cm^{-1} in SDD is assigned as the stretching mode of C_{20}=O_{21}. According to literature [31] the stretching mode of C=O is expected in the range 1850-1550 cm^{-1}. The in-plane bending mode of C=O is reported in the range 725 ± 95 cm^{-1} [26]. The C=O out of plane vibration is reported in the region 595 ± 120 cm^{-1} [26]. The C_{20}=O_{21} deformation bands are assigned at 704 and 514 cm^{-1} theoretically (SDD).

In the following discussion the mono-substituted and 1,2-disubstituted benzene ring are labelled as PhII and PhI respectively. The quinoline has been labelled as ring. For 1,2 light/heavy di-substituted benzenes, the C-H stretching modes of the phenyl ring are expected in the region 3100-3000 cm^{-1} [26] and for mono-substituted benzenes, these modes are expected in the region 3105-3000 cm^{-1} [26]. For the title compound these modes are observed at 3168, 3085 cm^{-1} (IR), 3149 cm^{-1} (Raman) and in the range 3124-3069 cm^{-1} (SDD) theoretically.

The in-plane deformation modes are seen in the range 1300-1240 cm^{-1} and 1170-1010 cm^{-1} for 1,2 light/heavy di-substituted benzenes [26] where δC-H vibrations are seen in the range 1230-1280 $cm^{-1}$and 1170-1000 cm^{-1} for mono-substituted benzenes [26]. For the title compound these modes are observed at 1248, 1115 cm^{-1} (IR), 1253, 1114 cm^{-1} (Raman) and 1235, 1246, 1163, 1103 cm^{-1} (SDD) for di-substituted benzenes and at 1071 cm^{-1} (IR), 1177, 1150 cm^{-1} (Raman), 1328, 1177, 1160, 1068, 1014 cm^{-1} (SDD) for mono-substituted benzenes. The out-of-plane C-H deformation bands are expected in the region 995-720 cm^{-1} [26] and 1000-700 cm^{-1} [26, 30] for the di-substituted and mono-substituted benzenes respectively. These modes are observed at 865 cm^{-1} in IR, 944, 862 cm^{-1} in Raman and 992, 957, 868, 771 cm^{-1} in SDD for the di-substituted benzene and at 937, 792 cm^{-1} (IR), 1000, 848 cm^{-1} (Raman) 1000, 985, 929, 848, 774 cm^{-1} (SDD) for the mono-substituted benzene.

The benzene ring possesses six ring stretching vibrations with sixth is the ring breathing mode. The υPh modes are expected in the region of 1615-1270, 1620-1285 cm^{-1} for PhI, PhII rings, respectively [26]. Panicker et al., [36] reported this mode in the range of 1593-1011 cm^{-1} theoretically for PhI, where the ring stretching modes of PhII are reported [36] in the range 1599-1086 cm^{-1}. The modes at 1449 cm^{-1} (IR), 1457 cm^{-1} (Raman) 1593, 1547, 1445, 1347, 1235 cm^{-1} (SDD) and 1402 cm^{-1} (IR) 1585, 1413, 1334 cm^{-1} (Raman) 1587, 1560, 1469, 1424, 1333 cm^{-1} (SDD) are assigned as the ring stretching modes of PhI and PhII, respectively. In ortho di-substitution the ring breathing mode has three wavenumber

intervals depending on whether both substituents are heavy, or one of them is heavy, while the other is light, or both of them are light. In the first case, the interval is 1100-1130 cm^{-1}, in the second case 1020-1070 cm^{-1}, while in the third case it is between 630-780 cm^{-1} [30]. For mono-substituted benzenes the ring breathing mode is observed about 1000 cm^{-1} [26]. For the title compound the modes at 1030 cm^{-1} (IR), 1030 cm^{-1} (Raman) 1022 cm^{-1} (SDD) and at 1009 cm^{-1} (SDD) are assigned as the ring breathing mode for PhI and PhII, respectively.

The C-H stretching outside the ring shows the bands at 3062, 3029 cm^{-1} (IR), 3067, 3030 cm^{-1} (Raman) and 3068, 3053 cm^{-1} (SDD). These bands are expected in the general region 3000-2840 cm^{-1} [34]. The in-plane and out-of-plane bending vibrations of the C-H are also observed at 1305 cm^{-1} and 882 cm^{-1} theoretically and these vibrations are expected in the regions 1350-1150 cm^{-1} and 1000-650 cm^{-1} [26, 34].

The C=C stretching is reported [37] in the IR spectrum around 1610 cm^{-1} and at 1609 cm^{-1} in Raman spectrum, where we have assigned this mode at 1606 in IR , 1601 in Raman and 1608 cm^{-1} in SDD. Arjunan et al. [37] reported the C-C stretching at 1281 and 1334 cm^{-1} (IR) ,1271 and 1384 cm^{-1} in Raman, where we observed this mode at 1268 and 1305 cm^{-1} in SDD, and the latter mode has contributions from other modes too. The C-N stretching is observed at 1248 cm^{-1} (IR), 1319, 1253 cm^{-1} (Raman), 1323, 1246 cm^{-1} (SDD) while C-N stretching is reported [37] at 1205 cm^{-1}. Another C=O stretching mode is theoretically observed at 1577 cm^{-1} which is in agreement with the reported values for similar quinoline derivatives [38]. For Quinoline ring, C-Cl stretching absorption is observed in the broad region between 850 and 550 cm^{-1} [39, 31]. Arjunan et al. [37] reported C-Cl stretching at 734 cm^{-1} (IR), 735 cm^{-1} (Raman), in-plane bending at 505 cm^{-1} (IR) 497 cm^{-1} (Raman) and out-of-plane at 263 cm^{-1} where we have assigned these modes at 576, 383, 220 cm^{-1} theoretically (SDD) for the title compound.

In order to investigate the performance of vibrational wavenumbers of the title compound, root mean square (RMS) values of wavenumbers were calculated using the expression, RMS = $\sqrt{\left(\frac{1}{n-1}\right)\sum_i^n \left(\nu_i^{calc} - \nu_i^{exp}\right)^2}$.The RMS error of the observed IR bands and Raman bands were found to be 28.01 (HF/6-31G(6D,7F)), 31.96 (B3LYP/6-31G(6D,7F)), 12.82 (B3LYP/SDD) and 26.86 (HF/6-31G(6D,7F)), 25.45 (B3LYP/6-31G(6D, 7F)), 9.43 (B3LYP/SDD), respectively. The small difference between experimental and calculated vibrational modes may be due to the fact that experimental results belong to the solid phase and theoretical calculations belong to gaseous phase.

4.2 Optimized geometrical parameters

For the title compound, the computationally obtained bond lengths are, C_3-C_4 = 1.3986, C_4-C_5 = 1.4124, C_4-H_{10} = 1.088, C_5-N_{11} = 1.398, C_6-C_{15} = 1.4539, C_{13}-C_{17} = 1.4828, C_{15}-Cl_{16} = 1.8083, C_{15}-C_{17} = 1.3754, N_{18}-H_{19} = 1.0194, N_{18}-C_{20} = 1.4089, C_{20}-O_{21} = 1.2546, C_5-C_6=1.4263Å, while the reported values are 1.3806, 1.4211, 1.0841, 1.3725, 1.417, 1.415, 1.7329, 1.375, 1.0161, 1.3826, 1.2538, 1.435Å [36, 38, 40, 41]. The bond lengths of C_5-N_{11} (1.398Å) and C_{20}-N_{18} (1.4089Å) are shorter than the normal C-N bond length of about 1.48Å. This points in to the effect of resonance in this part of the molecule [42]. The shortening of the bond length of C_{20}-O_{21} (1.2546Å) and C_{13}-O_{14} (1.2653Å) could be assigned a double bond character. The longer bond length of C_5-C_6 (1.4263Å) is due to the delocalization of electron density due to the presence of nearby quinoline ring.

The observed bond angles are C_4-C_5-C_6 = 120.7°, C_1-C_6-C_5 = 118.3°, C_1-C_6-C_{15} = 124.1°, C_5-N_{11}-C_{13} = 125.3°, N_{11}-C_{13}-C_{17} = 116.0°, C_6-C_{15}-Cl_{16} = 117.6°, C_6-C_{15}-C_{17} = 122.1°, C_{13}-C_{17}-C_{15} = 119.6°, H_{19}-N_{18}-C_{20} = 116.7°, N_{18}-C_{20}-O_{21} = 122.6°, while the reported values are 120.2°, 119.5°, 123.6°, 118.6°, 123.6°, 119.5°, 119.7°, 119.2°, 120.6°, 121.4° [36, 38, 40, 41]. The large bond angle value of C_6-C_{15}-C_{17} (122.1°) is due to the presence of chlorine, which is highly electronegative and would draw electron density from neighbouring atoms [43]. The lesser bond angle value of C_1-C_6-C_5 (118.3°) is understood as due to the presence of quinoline ring because for a benzene ring each C-C-C angle is 120°. It is seen that the N_{11}-C_{13}-O_{14} bond angle (121.8°) is considerably greater than the N_{11}-C_{13}-C_{17} angle (116.0°), which is explained as due to a decrease in the repulsion between the lone pairs present in N_{11} and O_{14} atoms [44]. The dihedral angle H_{19}-N_{18}-C_{20}-O_{21} is reported as 172.0° [38], while we observe this at -157.0° which denoted a tilting from the plane.

4.3 Nonlinear optical properties

The first hyperpolarizability (β_0) of this novel molecular system is calculated using the SDD method, based on the finite-field approach. In the presence of an applied electric field, the energy of a system is a function of the electric field. The first hyperpolarizability is a third-rank tensor that can be described by a 3×3×3 matrix. The 27 components of the 3D matrix can be reduced to 10 components due to the Kleinman symmetry [45] .The components of β are defined as the coefficients in the Taylor series expansion of the energy in the external electric field. When the electric field is weak and homogeneous, this expansion become

$$E = E_0 - \sum_i \mu_i F^i - \frac{1}{2}\sum_{ij} \alpha_{ij} F^i F^j - \frac{1}{6}\sum_{ijk} \beta_{ijk} F^i F^j F^k - \frac{1}{24}\sum_{ijkl} \gamma_{ijkl} F^i F^j F^k F^l + \ldots$$

where E_0 is the energy of the unperturbed molecule, F^i is the field at the origin, μ_i, α_{ij}, β_{ijk} and γ_{ijkl} are the components of dipole moment, polarizability, the first hyperpolarizabilities, and second hyperpolarizabilities, respectively.

$\beta_0 = (\beta_x^2 + \beta_y^2 + \beta_z^2)^{1/2}$

where

$\beta_x = \beta_{xxx} + \beta_{xyy} + \beta_{xzz}$

$\beta_y = \beta_{yyy} + \beta_{xxy} + \beta_{yzz}$

$\beta_z = \beta_{zzz} + \beta_{xxz} + \beta_{yyz}$

The calculated first hyperpolarizability of the title compound is 16.9×10^{-30} esu which is 130 times that of standard NLO material urea (0.13×10^{-30} esu) [46]. The first hyperpolarizability of quinoline derivatives is reported as 2.24×10^{-30} esu and 2.39×10^{-30} esu [40, 47]. But experimental evaluation of this data is not readily available. We conclude that the title compound is an attractive object for future studies of nonlinear optical properties.

4.4 HOMO and LUMO

The HOMO (Highest Occupied Molecular Orbital) and LUMO (Lowest Unoccupied Molecular Orbital) are named as frontier molecular orbital (FMO). FMOs play an important role in optical and electrical properties, as well as in quantum chemistry. The conjugated molecules are characterized by a HOMO-LUMO separation, which is the result of a significant degree of intra-molecular charge transfer from the end-capping electron-donor groups to the efficient electron-acceptor groups through π-conjugated path. The strong charge transfer interaction through π-conjugated bridge results in substantial ground state donor-acceptor mixing and the appearance of a charge transfer band in the electronic absorption spectrum (Fig. 4). The energy gap between the HOMO and LUMO energy is basis for molecular chemical stability, chemical reactivity and hardness-softness of the molecule [48]. The energy gap is found to be 2.23eV.

4.5 Molecular Electrostatic Potential

MEP is related to the electron density and is a very useful descriptor in understanding sites for electrophilic and nucleophilic reactions as well as hydrogen bonding interactions [49, 50]. The electrostatic potential V(r) is also well suited for analyzing processes based on the "recognition" of one molecule by another, as in drug-receptor, and enzyme-substrate interactions, because it is through their potentials that the two species first "see" each other

[51, 52]. To predict reactive sites of electrophilic and nucleophilic attacks for the investigated molecule, MEP at the B3LYP/SDD optimized geometry was calculated. The negative (red and yellow) regions of MEP were related to electrophilic reactivity and the positive (blue) regions to nucleophilic reactivity (Fig. 5). From the MEP it is evident that the negative charge covers the carbonyl group and the positive region is over the NH group. The more electro negativity in the carbonyl group makes it the most reactive part in the molecule.

4.6. Natural bond orbital analysis

The natural bond orbital (NBO) calculations were performed using NBO 3.1 program [53] as implemented in the Gaussian09 package at the B3LYP/SDD level in order to understand various second-order interactions between the filled orbital of one subsystem and vacant orbital of another subsystem, which is a measure of the intra-molecular delocalization or hyper-conjugation. NBO analysis provides the most accurate possible 'natural Lewis structure' picture of 'j' because all orbital details are mathematically chosen to include the highest possible percentage of the electron density. A useful aspect of the NBO method is that it gives information about interactions of both filled and virtual orbital spaces that could enhance the analysis of intra- and inter-molecular interactions. The second-order Fock-matrix was carried out to evaluate the donor-acceptor interactions in the NBO basis. The interactions result in a loss of occupancy from the localized NBO of the idealized Lewis structure into an empty non- Lewis orbital. For each donor (i) and acceptor (j) the stabilization energy (E2) associated with the delocalization i → j is determined as

$$E(2) = \Delta E_{ij} = q_i \frac{(F_{i,j})^2}{(E_j - E_i)}$$

q_i →donor orbital occupancy, E_i, E_j→diagonal elements, F_{ij} →the off diagonal NBO Fock matrix element.

In NBO analysis large E (2) value shows the intensive interaction between electron-donors and electron- acceptors, and greater the extent of conjugation of the whole system, the possible intensive interaction are given in Table 3. The second-order perturbation theory analysis of Fock-matrix in NBO basis shows strong intra-molecular hyper-conjugative interactions are formed by orbital overlap between n(Cl), n(O) and π*(C-C), σ*(C-N), bond orbital which result in ICT causing stabilization of the system. There occurs an intra-molecular hyper-conjugative interaction of C_{13}-N_{11} from O_{14} of $n_2(O_{14})$→ σ*(C_{13}-N_{11}) which increases ED(0.06847e) that weakens the respective bonds C_{13}-N_{11} leading to stabilization of 21.92 kJ/mol. Another hyper-conjugative interaction of C_{15}-C_{17} from Cl_{16} of $n_2(Cl_{16})$→

$\pi^*(C_{15}\text{-}C_{17})$ which increases ED (0.29246e) that weakens the respective bonds $C_{15}\text{-}C_{17}$ leading to stabilization of 12.68 kJ/mol. Another strong hyper-conjugative interaction of $C_{20}\text{-}N_{18}$ from O_{21} of $n_2(O_{21})\rightarrow\sigma^*(C_{20}\text{-}N_{18})$ which increases ED (0.08318e) that weakens the respective bonds $C_{20}\text{-}N_{18}$ leading to stabilization of 25.5 kJ/mol. These interactions are observed as an increase in electron density in C-C orbital that weakens the respective bonds.

The increased electron density at the oxygen, nitrogen and chlorine atoms leads to the elongation of respective bond length and a lowering of the corresponding stretching wave number. The electron density is transferred from the n(N) to the anti-bonding π* orbital of the C-C and C-O bonds, and also from n(Cl) to the anti-bonding π* orbital of the C-C explaining both the elongation and the red shift [54].The hyper-conjugative interaction energy was deduced from the second-order perturbation approach. Delocalization of electron density between occupied Lewis-type (bond or lone pair) NBO orbital and formally unoccupied (anti bond or Rydberg) non-Lewis NBO orbitals corresponds to a stabilizing donor-acceptor interaction. The NH and C=O stretching modes can be used as a good probe for evaluating the bonding configuration around the atoms and the electronic distribution in the ring. Hence the title compound is stabilized by these orbital interactions.

The NBO analysis also describes the bonding in terms of the natural hybrid orbital $n_2(O_{14})$, which occupy a higher energy orbital (-0.26770a.u.) with considerable p-character (99.99%) and low occupation number (1.87789) and the other $n_1(O_{14})$ occupy a lower energy orbital(-0.69816a.u.) with p-character (34.55%) and high occupation number (1.97573). The NBO analysis also describes the bonding in terms of the natural hybrid orbital $n_3(Cl_{16})$, which occupy a higher energy orbital (-0.31704a.u.) with considerable p-character (99.90%) and low occupation number (1.92) and the other $n_2(Cl_{16})$ occupy a lower energy orbital (-0.32163a.u.) with p-character (99.70%) and high occupation number (1.97019). The NBO analysis also describes the bonding in terms of the natural hybrid orbital $n_2(O_{21})$, which occupy a higher energy orbital (-0.24881a.u.) with considerable p-character (99.98%) and low occupation number (1.87847) and the other $n_1(O_{21})$ occupy a lower energy orbital (-0.67333a.u.) with p-character (36.17%) and high occupation number (1.97550). Thus, a very close to pure p-type lone pair orbital participates in the electron donation to the $\pi^*(C_{13}\text{-}O_{14})$ orbital for $n_1(N_{11})\rightarrow\pi^*(C_{13}\text{-}O_{14})$, $\sigma^*(C_{13}\text{-}C_{17})$ orbital for $n_1(O_{14})\rightarrow\sigma^*(C_{13}\text{-}C_{17})$, $\sigma^*(C_{13}\text{-}N_{11})$ orbital for $n_2(O_{14})\rightarrow\sigma^*(C_{13}\text{-}N_{11})$, $\sigma^*(C_6\text{-}C_{15})$ orbital for $n_1(Cl_{16})\rightarrow\sigma^*(C_6\text{-}C_{15})$, $\pi^*(C_{15}\text{-}C_{17})$ orbital for $n_2(Cl_{16})\rightarrow\pi^*(C_{15}\text{-}C_{17})$, $\pi^*(C_{20}\text{-}O_{21})$ orbital for $n_1(N_{18})\rightarrow\pi^*(C_{20}\text{-}O_{21})$, $\sigma^*(C_{20}\text{-}C_{22})$

orbital for $n_1(O_{21})\rightarrow\sigma^*(C_{20}\text{-}C_{22})$, $\sigma^*(C_{20}\text{-}N_{18})$ orbital for $n_2(O_{21})\rightarrow\sigma^*(C_{20}\text{-}N_{18})$interactions in the compound. The results are tabulated in Table 4.

4.7 Mulliken Charges

The calculation of atomic charges plays an important role in the application of quantum mechanical calculations to molecular systems. Mulliken charges are calculated by determining the electron population of each atom as defined in the basis of functions. The charge distributions calculated by the Mulliken [55] and NBO methods for the equilibrium geometry of the title compound are given in Table 5. The charge distribution on the molecule has an important influence on the vibrational spectra. In the title compound, the distribution of Mulliken atomic charge shows the direction of delocalization and shows that the natural atomic charges are more sensitive to the changes in the molecular structure than Mulliken's net charges. Also we have done a comparison of Mulliken charges obtained by different basic sets and tabulated it in Table 6 in order to assess the sensitivity of the calculated charges to changes in (i) the choice of the basis set; (ii) the choice of the quantum mechanical method. The results can, however, better be represented in graphical form as shown in Fig. 6. We have observed a change in the charge distribution by changing different basis sets. Distribution of the charges in this compound is also influenced by the C-O moieties. Based on the charge distribution calculated by various ways (see Tables 5 and 6) it can be concluded that all the hetero atoms showed significant electron density. An increased electron density (negative charge) can be also found at C_{17}, C_{22}, N_{11} and N_{18}. Significantly positive charges were predicted for C_{13}, and C_{20}. Therefore it can be concluded that electrophilic substitution of the quinoline scaffold is more preferred than nucleophilic substitution. Reactions based on the attack of a nucleophile are favoured especially on carbonyl/carboxyl carbons (C_{13}, C_{20}).

4.8 PES scan studies

For the dihedral angles $C_{15}\text{-}C_{17}\text{-}N_{18}\text{-}H_{19}$ and $C_{15}\text{-}C_{17}\text{-}N_{18}\text{-}C_{20,}$ a detailed potential energy surface (PES) scan has been performed at B3LYP/SDD level to reveal all possible conformations of the title compound. The PES scan was carried out by minimizing the potential energy in all geometrical parameters by changing the torsion angle at every 10˚ for 180˚ rotation around the bond. The results obtained in PES scan study by varying the torsion perturbation around the above dihedral angles are plotted in Fig. 7 and Fig. 8. For the $C_{15}\text{-}C_{17}\text{-}N_{18}\text{-}H_{19}$ rotation, the minimum energy was obtained at -153.6˚in the potential energy curve of energy -1413.7549 Hartrees. For the $C_{15}\text{-}C_{17}\text{-}N_{18}\text{-}C_{20}$ rotation, the minimum energy occurs at 51.1˚ in the potential energy curve of energy -1413.7550 Hartrees.

4.9. ^{1}H-NMR spectrum

Using TMS as internal standard, experimental spectrum data of the title compound in DMSO is obtained at 500 MHz and is shown in Table 7. The absolute isotropic chemical shielding of the title compound was calculated by B3LYP/GIAO model [56]. Relative chemical shifts were then estimated by using the corresponding TMS shielding: σ_{calc}(TMS) calculated in advance at the same theoretical level as this paper. Numerical values of chemical shift $\delta_{calc} = \sigma_{calc}(TMS) - \sigma_{calc}$ together with calculated values of σ_{calc} (TMS), are reported in Table 7. The chemical shift and the experimental ^{1}H-NMR data were in agreement. Thus, the results have shown that the predicted proton chemical shifts were in good agreement with the experimental data for the title compound.

4.10. Molecular docking

Quinolones constitute a series of broad-spectrum antibacterial drugs [57]. Extensive literature survey reveals that quinole derivatives mostly possess antimicrobial activity [58-60]. From this background knowledge we decided to evaluate antimicrobial potential of the quinoline derivative. With time most microbs develop resistance against antimicrobial drugs. This leads to an ever increasing demand for the development of new antimicrobial agents. As mycobacterium tuberculosis is the leading bacterial infection in the world [61] so we decided to carry molecular docking simulations against targets from *mycobacterium tuberculosis*. The *Mycobacterium tuberculosis* genome contains 11 serine/threonine kinase genes including PknA and PknB, which play vital role in cell shape control and cell wall synthesis. PknB, a receptor-like protein kinase is essential for myco-bacterial viability. PknB is predominant in many more distantly related gram-positive bacteria [62, 63]. Molecular docking simulations were performed on AutoDock-Vina software [64]. The 3D crystal structure of *M. tuberculosis* PknB was obtained from Protein Data Bank (PDB ID: 2FUM) [65]. The protein was prepared for docking by removing the co-crystallized ligand, water molecules and co-factors. Auto Dock Tools (ADT) graphical user interface was used to calculate Kollman charges and to add polar hydrogen. Ligand was prepared for docking by minimizing its energy at B3LYP/SDD level of theory. Charges were calculated by Geistenger method. Active site of the protein was defined so as to include residues of the active site within the grid size of 40Å×40Å×40Å. The most popular algorithm, Lamarckian Genetic Algorithm (LGA) available in Autodock was employed for docking. Docking protocol was tested by extracting co-crystallized inhibitor from the protein and then docking the same. Docking protocol which we employed predicted the same conformation as was present in the crystal

structure with RMSD value well within the reliable range of 2Å. Amongst the docked conformations, one which binds at the active site with high affinity was visualized for detailed ligand-protein interactions in Discover Studio Visualizer 4.0 and Pymol software. The ligand binds at the catalytic site of substrate (Fig. 9) by weak non-covalent interactions most prominent of which are H-bonding and alkyl-π interactions.Val95 form H-bonds of 2.68Å length with carbonyl oxygen attached to quinoline ring. Val72, Val25 and Leu17 hold the aromatic rings by alkyl-π interactions (supporting information Fig.S1). The inhibitor (2*E*)-*N*-(4-chloro-2-oxo-1,2-dihydroquinolin-3-yl)-3-phenylprop-2-enamide forms a stable complex with PknB as is evident from the binding affinity (ΔG in kcal/mol) values (supporting material Table S1). These preliminary results suggest that the compound might exhibit inhibitory activity against PknB. This may result in development of new anti-tuberculostic agents. However biological tests need to be done so as to validate the computational predictions.

5. Conclusion

The vibrational spectroscopic studies of (2*E*)-*N*-(4-chloro-2-oxo-1,2-dihydroquinolin-3-yl)-3-phenylprop-2-enamide were reported experimentally and theoretically. Potential energy distribution of normal modes of vibrations was done using GAR2PED program. The ring stretching modes in IR and Raman spectra are evidence for charge transfer interaction between the donor and the acceptor group through the π system. This along with the lowering of HOMO-LUMO band gap supports for the bioactivity of the molecule. NBO analysis predicts a strong intra-molecular hyper conjugative interaction of (C_{13}-O_{14}) from N_{11} of $n_1(N_{11})$, (C_{13}-C_{17}) from O_{14} of $n_1(O_{14})$, (C_{13}-N_{11}) from O_{14} of $n_2(O_{14})$, (C_6-C_{15}) from Cl_{16} of $n_1(Cl_{16})$, (C_{15}-C_{17}) from Cl_{16} of $n_2(Cl_{16})$, (C_{20}-O_{21}) from N_{18} of $n_1(N_{18})$, (C_{20}-C_{22}) from O_{21} of $n_1(O_{21})$, (C_{20}-N_{18}) from O_{21} of $n_2(O_{21})$. MEP predicts the most reactive part in the molecule. The calculated first hyperpolarizability is comparable with the reported values of similar derivatives and is an attractive object for future studies in non-linear optics. The minimum energy surfaces are obtained from the potential energy curve by PES scan studies. In addition the calculated ^{1}H-NMR results are in good agreement with experimental data. The title compound, (2*E*)-*N*-(4-chloro-2-oxo-1,2-dihydroquinolin-3-yl)-3-phenylprop-2-enamide forms a stable complex with PknB as is evident from the binding affinity and molecular docking studies suggest that the compound might exhibit inhibitory activity against PknB.

Acknowledgements

The authors are thankful to University of Antwerp for access to the university's CalcUA supercomputer cluster. JAW would like to thank Department of Science and Technology, New Delhi, India for a INSPIRE fellowship and RTU thanks University of Kerala, India for a research fellowship. A.A.Al-Saadi thanks King Fahd University for Petroleum and Minerals for providing the computing facility to support this work.

References

[1] F. Hayat, A. Salahuddin, S. Umar, A. Azam, Eur. J. Med. Chem. 45 (2010) 4669-4675.

[2] L.M. Bedoya, M.J. Abad, E. Calonge, L.A. Saavedra, C.M. Gutierrez, V.V. Kouznetsov, J. Alcami, P. Bermejo, Antivir. Res. 87 (2010) 338-344.

[3] A.M. Asiri, A.O. Baglaf, R.M. Abdel-Rahman, S.A. Khan, M. Ishaq, Asian J. Chem. 25 (2013) 7779-7782.

[4] J. Zeigler, R. Linck, D.W. Wright, Curr. Med. Chem. 8 (2001) 171-189.

[5] P.M.S. Chauhan, S.K. Srivastava, Curr. Med. Chem. 8 (2001) 1535-1542.

[6] O. Famin, H. Krugliak, H.Ginsberg, Biochem. Pharmacol. 58 (1999) 59-68.

[7] F.M.D. Ismail, M.J. Dascombe, P. Carr, J. Pharm. Pharmacol. 50 (1998) 483-492.

[8] M.L. Go, T.L. Nigam, A.L.C. Tan, Eur. J. Pharm. Sci. 6 (1998) 19-26.

[9] A. Dorn, S.R. Vippagunda, H. Mitile, Biochem. Pharmacol. 55 (1998) 727-736.

[10] K. Singh, H. Kaur, K. Chibale, J. Balzarini, Eur. J. Med. Chem.66 (2013) 314-323.

[11] C.H. Chen, J.M. Shi, Coord. Chem. Rev. 171 (1998) 161-174.

[12] A.P. Kulkarni, J. Tonzola, A. Babel, S.A. Jenekhe, Chem. Mater. 16 (2004) 4556-4573.

[13] J. Park , J.S. Park , Y.G. Park , J.Y. Lee , J.W. Kang, J. Liu, L. Dai, S. Jin, Org. Electron. 14 (2013) 2114-2123.

[14] S. Yamaguchi, M. Goto, H. Takayanagi, H. Ogura, Bull. Chem. Soc. Jpn. 61 (1988) 1026-1028.

[15] P. Zaderenko, M.S. Gel, P. Lopez, P. Ballesteros, I. Fonseco, A. Albert, Acta Cryst. B53 (1997) 961-967.

[16] J. Jampilek, R. Musiol, M. Pesko, K. Kralova, M. Vejsova, J. Carroll, A. Coffey, J. Finster, D. Tabak, H. Niedbala, V. Kozik, J. Polanski, J. Csollei, J. Dohnal, Molecules 14 (2009) 1145-1159.

[17] V. Dolle, E. Fan, C.H. Nguyen, A. M. Aubertin, A. Kirn, M.L. Andreola, G. Jamieson, L. Tarrago-Litvak, E. Bisagni, J. Med. Chem. 38 (1995) 4679-4686.

[18] Gaussian 09, Revision B.01, M.J. Frisch, G.W. Trucks, H.B. Schlegel, G.E. Scuseria, M.A. Robb, J.R. Cheeseman, G. Scalmani, V. Barone, B. Mennucci, G.A. Petersson, H. Nakatsuji, M. Caricato, X. Li, H.P. Hratchian, A.F. Izmaylov, J. Bloino, G. Zheng, J.L. Sonnenberg, M. Hada, M. Ehara, K. Toyota, R. Fukuda, J. Hasegawa, M. Ishida, T. Nakajima, Y. Honda, O. Kitao, H. Nakai, T. Vreven, J.A. Montgomery, Jr., J.E. Peralta, F. Ogliaro, M. Bearpark, J.J. Heyd, E. Brothers, K.N. Kudin, V.N. Staroverov, T. Keith, R. Kobayashi, J. Normand, K. Raghavachari, A. Rendell, J.C. Burant, S.S. Iyengar, J. Tomasi, M. Cossi, N. Rega, J.M. Millam, M. Klene, J.E. Knox, J.B. Cross, V. Bakken, C. Adamo, J. Jaramillo, R. Gomperts, R.E. Stratmann, O. Yazyev, A.J. Austin, R. Cammi, C. Pomelli, J.W. Ochterski, R.L. Martin, K. Morokuma, V.G. Zakrzewski, G.A. Voth, P. Salvador, J.J. Dannenberg, S. Dapprich, A.D. Daniels, O. Farkas, J.B. Foresman, J.V. Ortiz, J. Cioslowski, D.J. Fox, Gaussian, Inc., Wallingford CT, 2010.

[19] J.B. Foresman, in: E. Frisch (Ed.), Exploring Chemistry with Electronic Structure Methods: A Guide to Using Gaussian, Gaussian, Inc., Pittsburg, PA, 1996.

[20] P.J. Hay, W.R. Wadt, J. Chem Phys. 82 (1985) 270-283.

[21] J. Zhao, Y. Zhang, L. Zhu, J. Mol. Struct. Theochem. 671 (2004) 179-187.

[22] GaussView, Version 5, R. Dennington, T. Keith, J. Millam, Semichem Inc., Shawnee Mission KS, 2009.

[23] J.M.L. Martin, C.V. Alsenoy, GAR2PED, A Program to Obtain a Potential Energy Distribution from a Gaussian Archive Record, University of Antwerp, Belgium, 2007.

[24] L.J. Bellamy, The IR spectra of complex molecules, John Wiley & sons, New York 1975.

[25] A. Spire, M. Barthes, H. Kallouai, G.D. Nunzio, Physics D 137 (2000) 392-396.

[26] N.P.G. Roeges, A guide to the complete interpretation of IR spectra of Organic Compounds, Wiley, New York 1994.

[27] Y.S. Mary, C.Y. Panicker, H.T. Varghese, K. Raju, T.E. Bolelli, I. Yildiz, M.C. Granadeiro, H.I.S. Nogueira. J. Mol. Struct 994 (2011) 223-231

[28] N.B. Colthup, L.H. Daly, S.E. Wiberly, Inroduction to Infrared and Raman Spectroscopy, third ed., Academic Press, Boston, 1990.

[29] A.S. El-Shahawy, S.M. Ahmed, N.K. Sayed, Spectrochim. Acta 66 (2007) 143-152.

[30] G. Varsanyi, Assignments of Vibrational Spectra of Seven Hundred Benzene Derivatives, Wiley, New York, 1974.

[31] G. Socrates, Infrared Characteristic Group Frequencies, John Wiley and Sons, New York, 1981.

[32] R. Minitha , Y.S. Mary, H.T. Varghese C.Y. Panicker, R. Ravindran, K. Raju, V.M. Nair, J. Mol. Struct. 985 (2011) 316-322.

[33] G. Louran, M. Lapkowski, S. Quillard, A. Pron, J.B. Buisson, S. Lefrant, J. Phys. Chem. 100 (1996) 6998-7006.

[34] R.M. Silverstein, F.X. Webster, Spectrometric Identification of Organic Compounds, sixth ed., John Wiley, Asia, 2003.

[35] H.T. Varghese, C.Y. Panicker, D. Philip, P. Pazdera, Spectrochim.Acta 67 (2007) 1055-1059.

[36] C.Y. Panicker, H.T. Varghese, K.R. Ambujakshan, S. Mathew, S. Ganguli, A.K. Nanda, C.V. Alsenoy, Eur. J. Chem. 1 (2010) 37-43.

[37] S. Arjunan, P. Mohan, C.V. Mythili, Spectrochim. Acta 72 (2009) 783-788.

[38] S.R. Sheeja, N.A. Mangalam, M.R.P. Kurup, Y.S. Mary, K. Raju , H.T. Varghese, C. Y. Panicker, J. Mol. Struct. 973 (2010) 36–46.

[39] M. Kurt, M. Yurdakul, S. Yurdakul, J. Mol. Struct. Theochem. 711 (2004) 25-32.

[40] A.J. Camargo, H.B. Napolitano, J.Z. Schpector, J. Mol. Struct. (Theochem.) 816 (2007) 145-151.

[41] Y. S. Mary, H. T. Varghese, C.Y. Panicker, M. Dolezal, Spectrochim.Acta 71 (2008) 725-730.

[42] H. Arslan, U. Florke, N. Kulcu, G. Binzet, Spectrochim. Acta 68 (2007)1347-1355.

[43] C.Y. Panicker, H.T. Varghese, V.S. Madhavan, S. Mathew, J. Vinsova, C. Van Alsenoy, Y.S Mary ,Y.S Mary; J. Raman Spectrosc. 40 (2009) 2176-2186.

[44] B.N.B. Raj, M.R.P. Kurup, E. Suresh, Spectrochim. Acta 71 (2008) 1253-1260.

[45] D.A. Kleinman, Phys. Rev. 126 (1962) 1977-1979.

[46] M. Adant, M. Dupuis, J.L. Bredas, Int. J. Quantum. Chem. 56 (1995) 497-507.

[47] G. Purohit, G.C. Joshi, Indian J. Pure Appl. Phys. 41 (2003) 922-927.

[48] D.F.V. Lewis, C. Ioannides, D.V. Parke, Xenobiotica 24 (1994) 401-408.

[49] E. Scrocco, J. Tomasi, Adv. Quantum. Chem. 103 (1978) 115-193.

[50] F.J. Luque, J.M. Lopez, M. Orozco, Theor. Chem. Acc. 103 (2000) 343-345.

[51] P. Politzer, J. S. Murray, in: Theoretical Biochemistry and Molecular Biophysics: A Comprehensive Survey, Vol. 2, Protein: D.L. Beveridge, R. Lavery, Eds., Adenine Press, Schenectady, NY, 1991, Chap. 13.

[52] E. Scrocco, J. Tomasi, Top. Curr. Chem. 42 (1973) 95-170.

[53] E.D. Glendening, A.E. Reed, J.E. Carpenter, F. Weinhold, NBO Version 3.1, Theoretical Chemistry Institute, University of Wisconsin, Madison, CI.

[54] J. Choo, S. Kim, H. Joo, Y. Kwon, J. Mol. Struct. (Theochem.) 587 (2002) 1-8.

[55] R.S. Mulliken, J. Chem. Phys., 23 (1955) 1833-1840.

[56] K. Wolinski, J.F. Hinton, P. Pulay, J. Am. Chem. Soc. 112 (1990) 8251-8260.

[57] M.I. Andersson, A.P. MacGowan, J. Antimicorb. Chemother. 51 (2003) 1-11.

[58] R. Wise, J.M. Andrews, J.P. Ashby, R.S. Matthews, Antimicrob. Agents Chemother. 32 (1988) 617-622.

[59] H.C. Neu, Annual Rev. Med. 43 (1992) 465-486.

[60] M.J. Pucci, J.A. Wiles, Bacterial Topoisomerase Inhibitors: Quinolones and Beyond, In Antimicrobials, ch.16, pp.307-326, Springer Berlin, Heidelber, 2014.

[61] M. Chhabria, P. Shailesh, J. Mitesh Anti-Infect. Agents Med. Chem. 9 (2010) 59-103.

[62] C.M. Kang, D.W. Abbott, S.T. Park, C.C. Dascher, L.C. Cantley, R.N. Husson, Genes Dev. 19 (2005) 1692-1704.

[63] P. Fernandez, B. Saint-Joanis, N. Barilone, M. Jackson, B. Gicquel, S.T. Cole, P.M. Alzari, J. Bacteriol. 188 (2006) 7778-7784.

[64] O. Trott, A. J. Olson, J. Comput. Chem. 31 (2010) 455-461.

[65] A. Wehenkel, P. Fernandez, M. Bellinzoni, V. Catherinot, N. Barilone, G. Labesse, M. Jackson, P.M. Alzari., FEBS Lett. 580 (2006) 3018-3022.

Figure Captions

Fig.1 FT-IR spectrum of (2*E*)-*N*-(4-chloro-2-oxo-1,2-dihydroquinolin-3-yl)-3-phenylprop-2-enamide

Fig.2 FT-Raman spectrum of (2*E*)-*N*-(4-chloro-2-oxo-1,2-dihydroquinolin-3-yl)-3-phenylprop-2-enamide

Fig.3 Optimized geometry (SDD) of (2*E*)-*N*-(4-chloro-2-oxo-1,2-dihydroquinolin-3-yl)-3-phenylprop-2-enamide

Fig.4 HOMO - LUMO plots of (2*E*)-*N*-(4-chloro-2-oxo-1,2-dihydroquinolin-3-yl)-3-phenylprop-2-enamide

Fig.5 MEP plot of (2*E*)-*N*-(4-chloro-2-oxo-1,2-dihydroquinolin-3-yl)-3-phenylprop-2-enamide

Fig.6. Comparison of different methods for calculated Mulliken charges

Fig.7. Profile of potential energy scans for the torsion angle C_{15}-C_{17}-N_{18}-H_{19}

Fig.8. Profile of potential energy scans for the torsion angle C_{15}-C_{17}-N_{18}-C_{20}

Fig.9 The docked conformation of the ligand binds at the catalytic site of PnkB. H bonds, sulphur-π and alkyl-π interactions are represented by green, brown and violet dotted lines, respectively. Hydrogen bonding pocket is shown for clarity

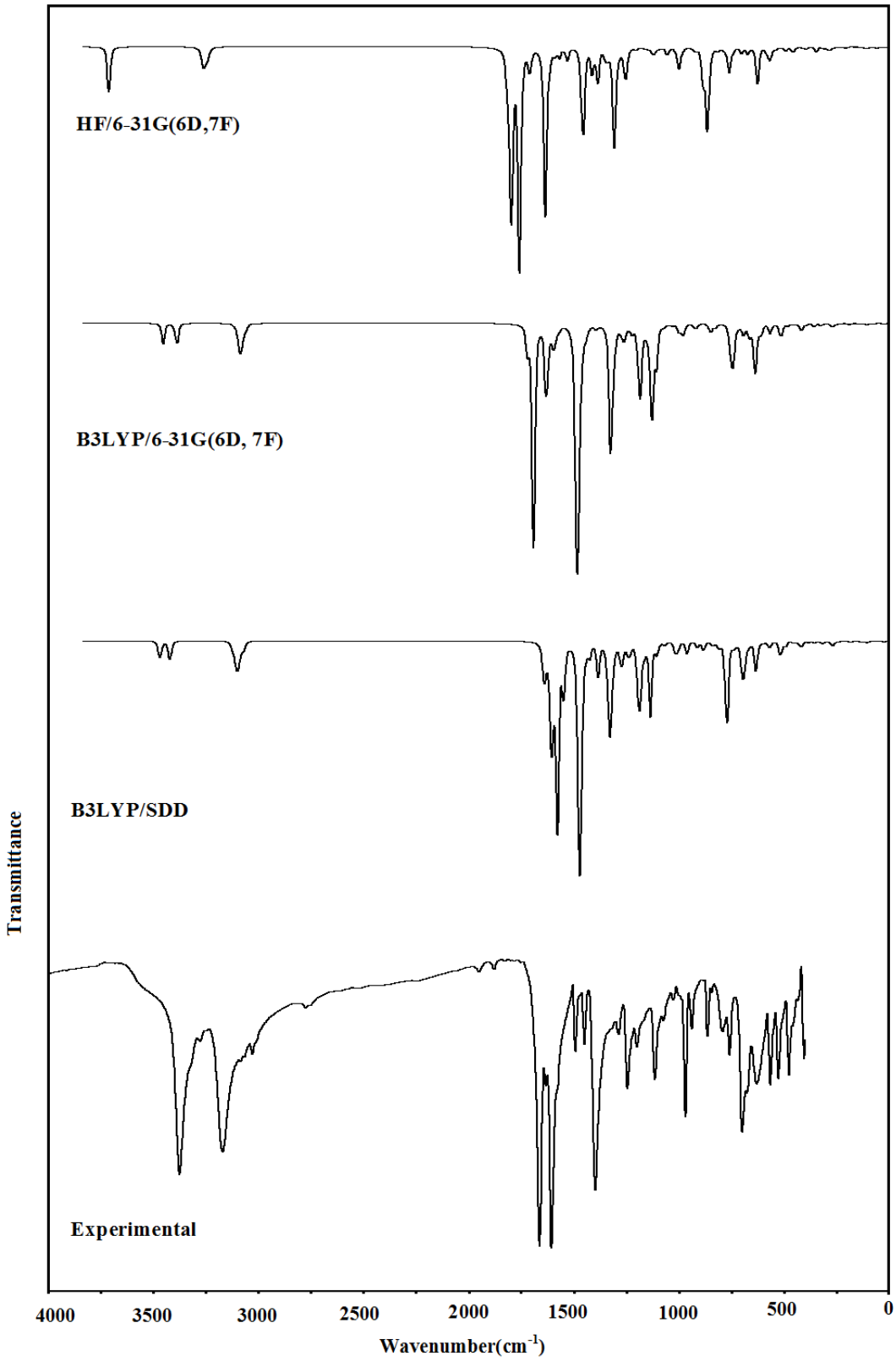

Fig.1 FT-IR spectrum of

(2*E*)-*N*-(4-chloro-2-oxo-1,2- dihydroquinolin-3-yl)-3-phenylprop-2-enamide

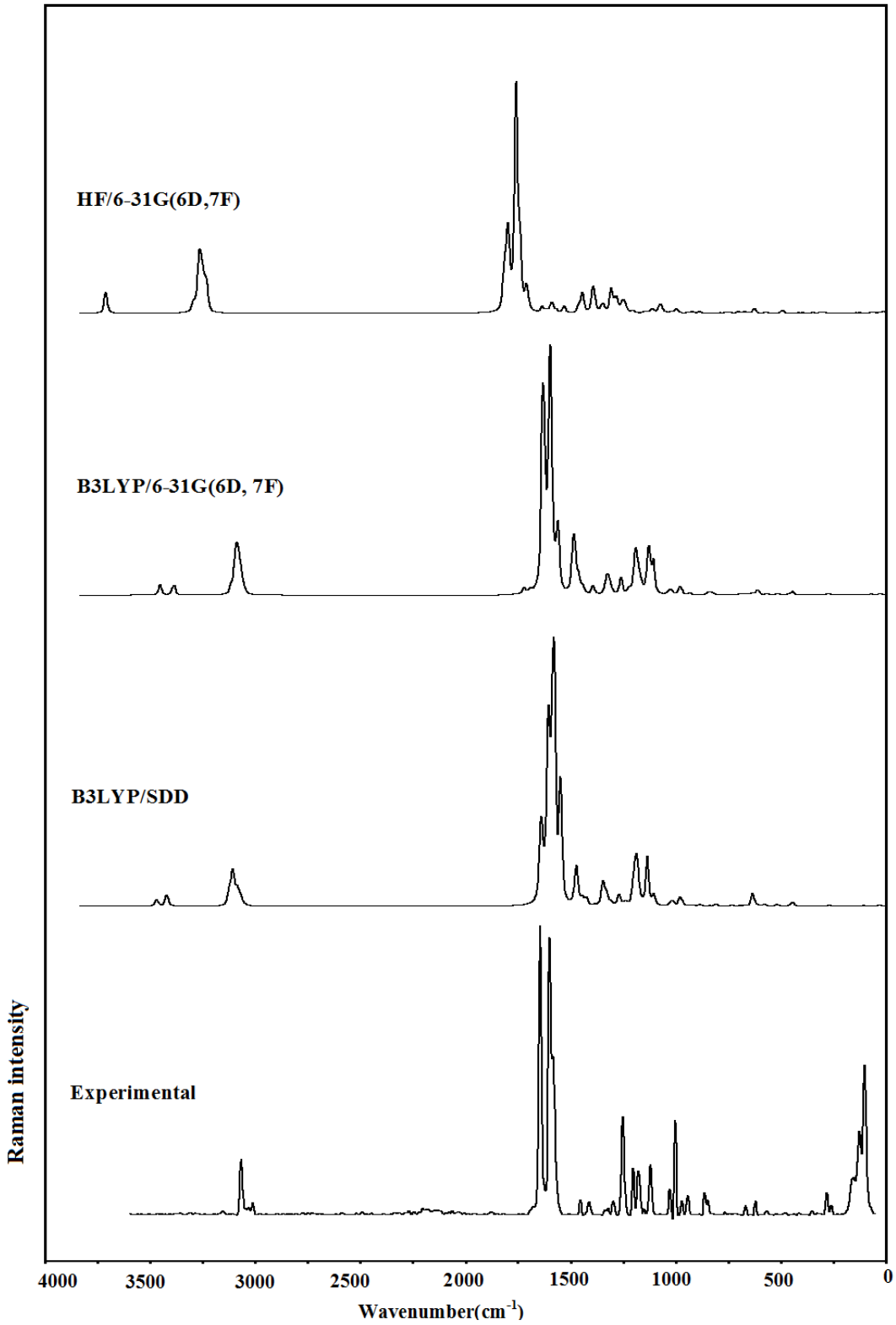

Fig.2 FT-Raman spectrum of

(2*E*)-*N*-(4-chloro-2-oxo-1,2-dihydroquinolin-3-yl)-3-phenylprop-2-enamide

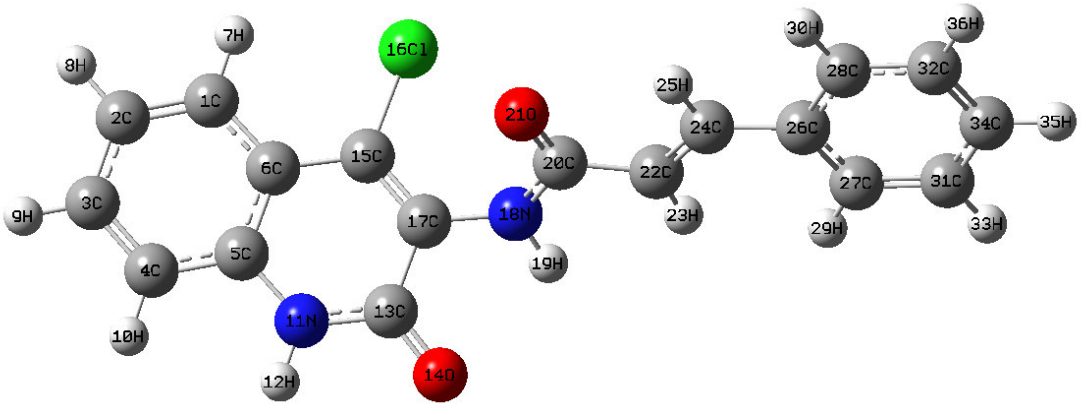

Fig.3 Optimized geometry (SDD) of
(2*E*)-*N*-(4- chloro-2-oxo-1,2-dihydroquinolin-3-yl)-3- phenylprop-2-enamide

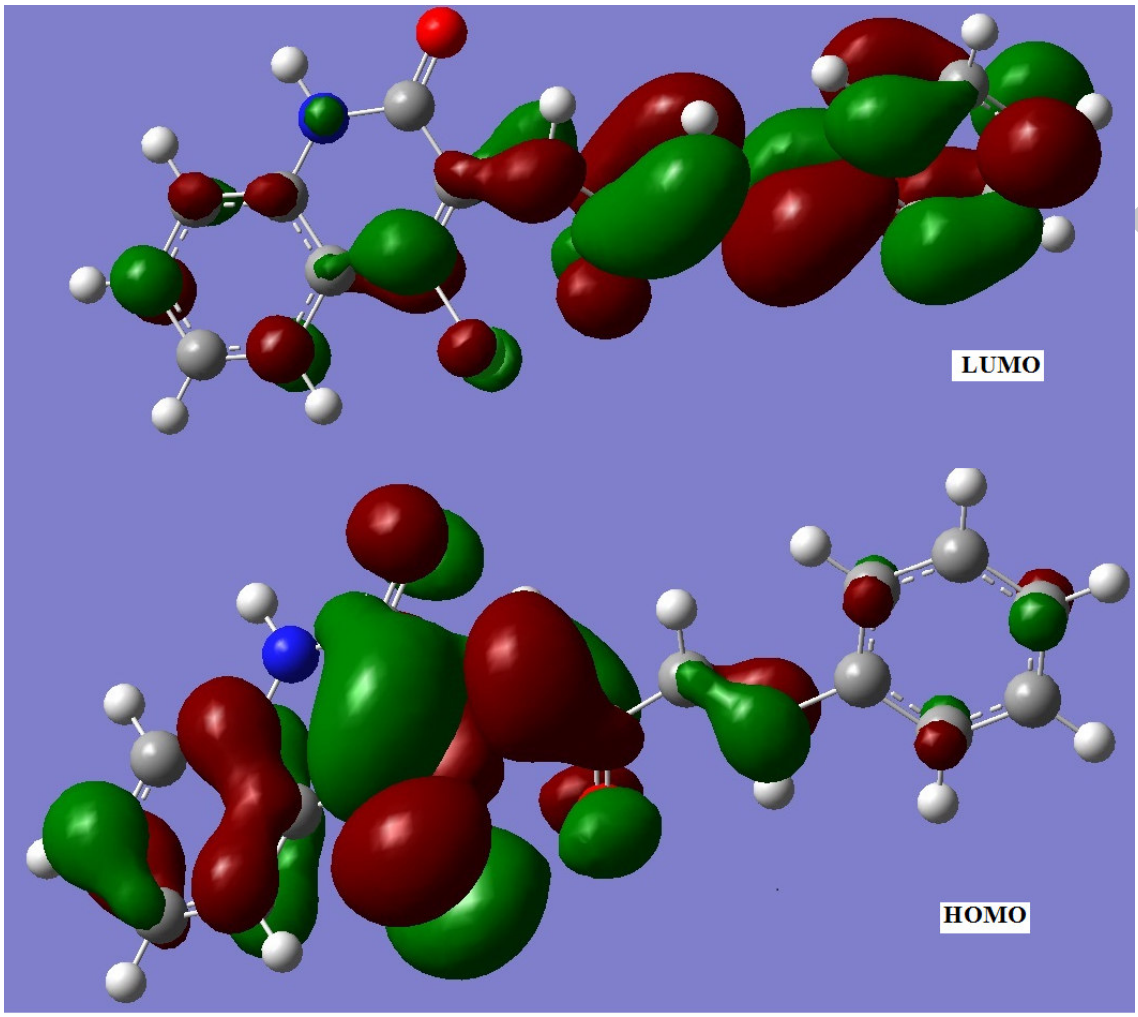

Fig.4 HOMO - LUMO plots of
(2*E*)-*N*-(4-chloro-2-oxo-1,2- dihydroquinolin-3-yl)-3-phenylprop-2-enamide

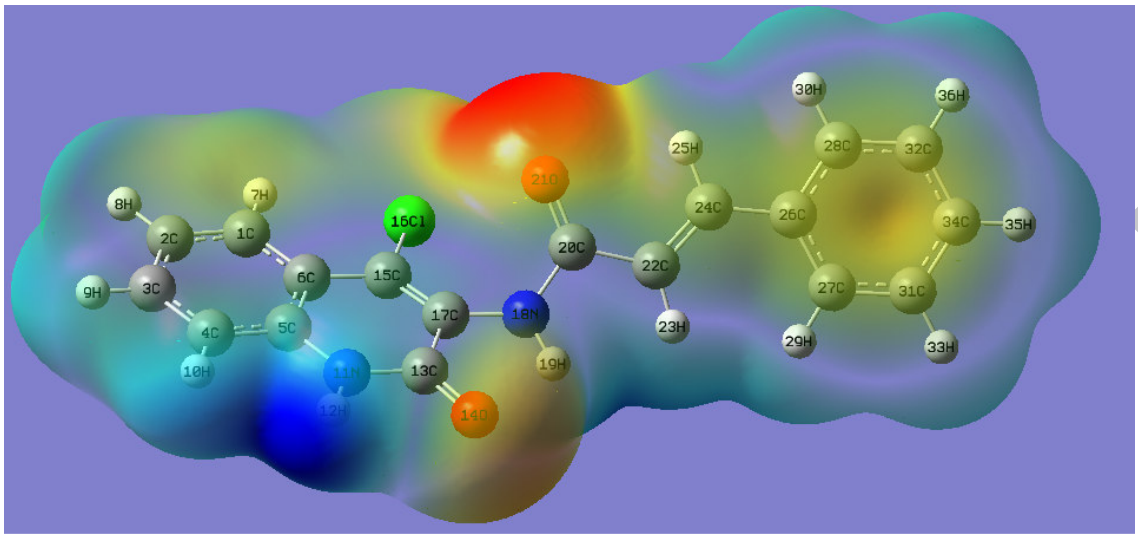

Fig.5 MEP plot of (2*E*)-*N*-(4-chloro-2-oxo-1,2-dihydroquinolin-3-yl)-3-phenylprop-2-enamide

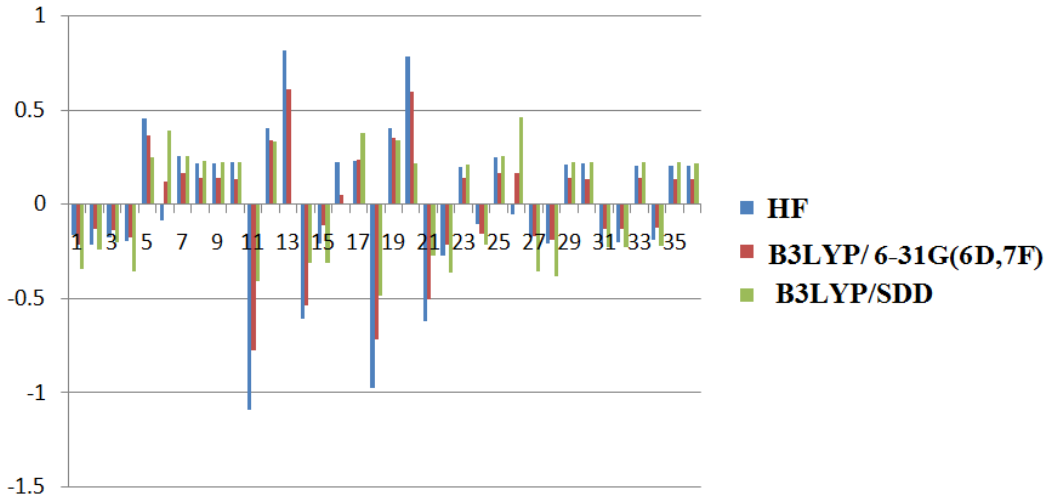

Fig.6. Comparison of different methods for calculated Mulliken charges

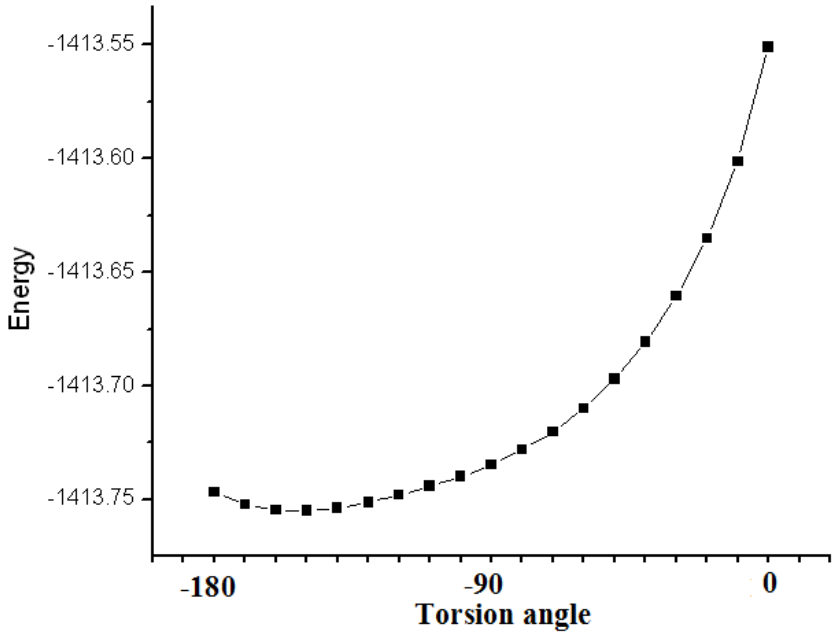

Fig.7. profile of potential energy scan for the torsion angle C_{15}-C_{17}-N_{18}-H_{19}

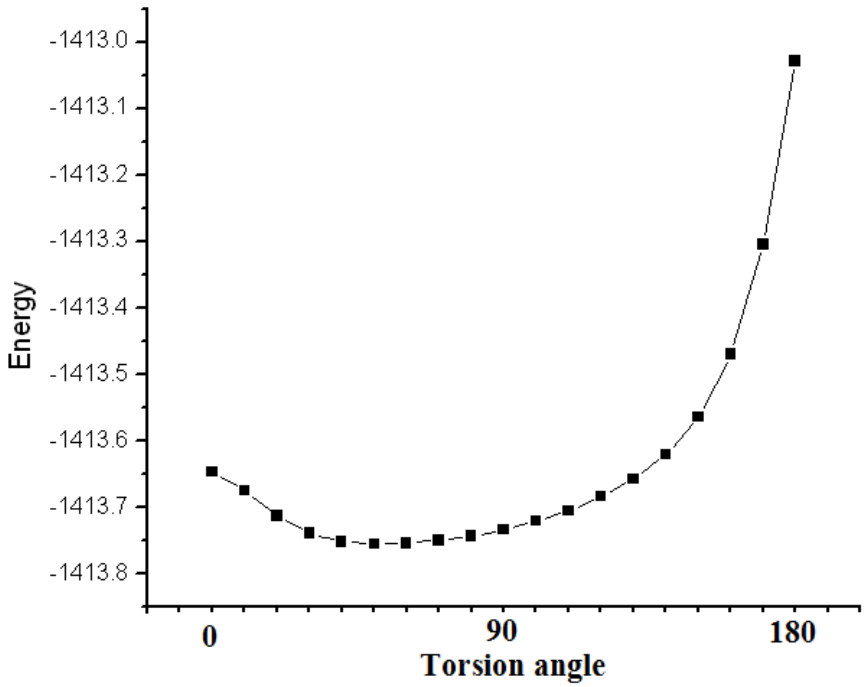

Fig.8. Profile of potential energy scan for the torsion angle C_{15}-C_{17}-N_{18}-C_{20}

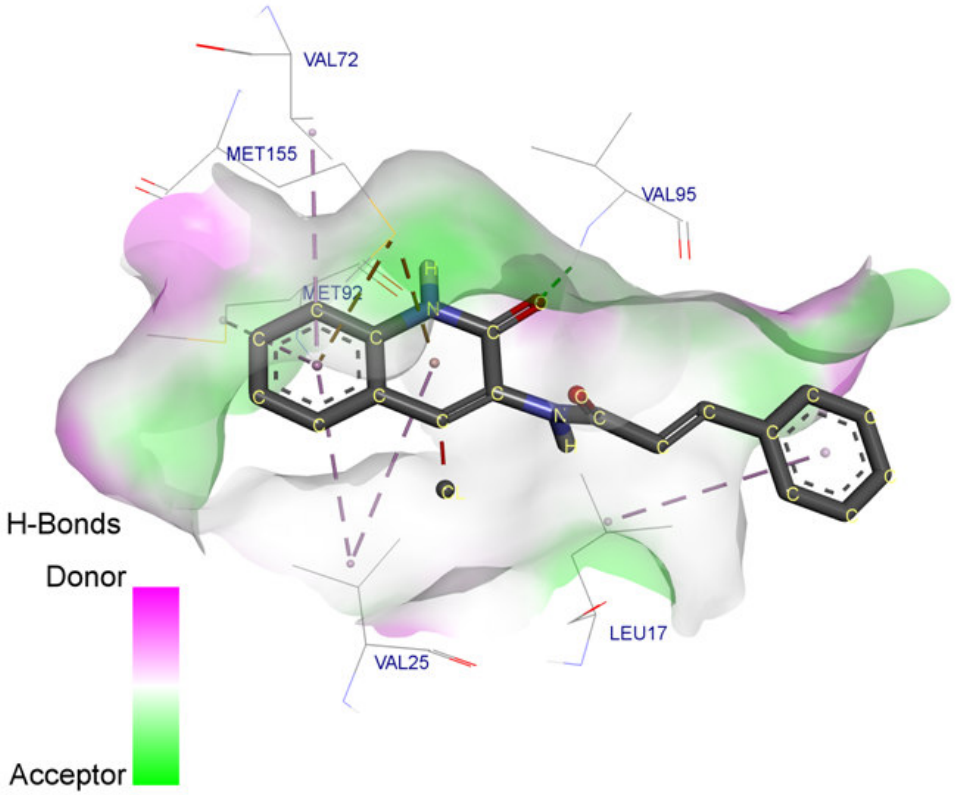

Fig.9 The docked conformation of the ligand binds at the catalytic site of PnkB. H bonds, sulphur-π and alkyl-π interactions are represented by green, brown and violet dotted lines, respectively. Hydrogen bonding pocket is shown for clarity

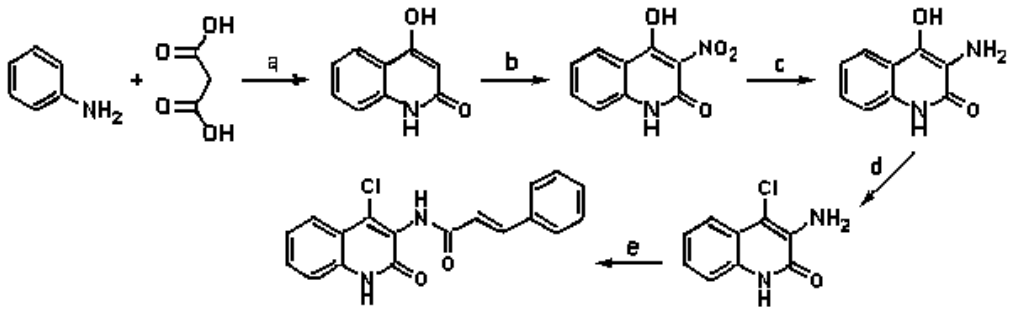

Scheme 1. Preparation of (2E)-N-(4-chloro-2-oxo-1,2-dihydroquinolin-3-yl)-3-phenylprop-2-enamide

Table 1.Optimized geometrical parameters (B3LYP/SDD) of (2*E*)-*N*-(4-chloro-2-oxo-1,2-dihydroquinolin-3-yl)-3-phenylprop-2-enamide, atom labeling according to Fig.3.

Bond lengths(Å)		Bond angles(°)		Dihedral angles(°)	
C1-C2	1.3976	C2-C1-C6	120.9	C6-C1-C2-C3	-0.1
C1-C6	1.4183	C2-C1-H7	120.2	C6-C1-C2-H8	179.8
C1-H7	1.0845	C6-C1-H7	118.9	H7-C1-C2-C3	-179.8
C2-C3	1.4156	C1-C2-C3	120.1	H7-C1-C2-H8	0.1
C2-H8	1.0861	C1-C2-H8	119.9	C2-C1-C6-C5	0.2
C3-C4	1.3986	C3-C2-H8	119.9	C2-C1-C6-C15	-180.0
C3-H9	1.0867	C2-C3-C4	120.1	H7-C1-C6-C5	179.9
C4-C5	1.4124	C2-C3-H9	120.1	H7-C1-C6-C15	-0.2
C4-H10	1.0880	C4-C3-H9	119.8	C1-C2-C3-C4	-0.1
C5-C6	1.4263	C3-C4-C5	119.8	C1-C2-C3-H9	179.9
C5-N11	1.3980	C3-C4-H10	120.5	H8-C2-C3-C4	-179.9
C6-C15	1.4539	C5-C4-H10	119.7	H8-C2-C3-H9	0.1
N11-H12	1.0164	C4-C5-C6	120.7	C2-C3-C4-C5	0.0
N11-C13	1.3861	C4-C5-N11	120.5	C2-C3-C4-H10	-179.9
C13-O14	1.2653	C6-C5-N11	118.8	H9-C3-C4-C5	-179.9
C13-C17	1.4828	C1-C6-C5	118.3	H9-C3-C4-H10	0.1
C15-Cl16	1.8083	C1-C6-C15	124.1	C3-C4-C5-C6	0.1
C15=C17	1.3754	C5-C6-C15	117.7	C3-C4-C5-N11	-178.9
C17-N18	1.4037	C5-N11-H12	119.4	H10-C4-C5-C6	-179.9
N18-H19	1.0194	C5-N11-C13	125.3	H10-C4-C5-N11	1.1
N18-C20	1.4089	H12-N11-C13	115.3	C4-C5-C6-C1	-0.3
C20=O21	1.2546	N11-C13-O14	121.8	C4-C5-C6-C15	179.9
C20-C22	1.485	N11-C13-C17	116.0	N11-C5-C6-C1	178.8
C22-H23	1.0884	O14=C13-C17	122.1	N11-C5-C6-C15	-1.0
C22=C24	1.3579	C6-C15-Cl16	117.6	C4-C5-N11-H12	1.9
C24-H25	1.091	C6-C15=C17	122.1	C4-C5-N11-C13	-178.0
C24-C26	1.4697	Cl16-C15=C17	0.0	C6-C5-N11-H12	-177.1
C26-C27	1.4195	C13-C17=C15	119.6	C6-C5-N11-C13	2.9
C26-C28	1.4177	C13-C17-N18	112.7	C1-C6-C15-Cl16	-7.2
C27-H29	1.0869	C15=C17-N18	127.5	C1-C6-C15-C17	175.5
C27-C31	1.4024	C17-N18-H19	112.8	C5-C6-C15-Cl16	172.6

C28-H30	1.0883
C28-C32	1.4053
C31-H33	1.0873
C31-C34	1.4115
C32-C34	1.4079
C32-H36	1.0871
C34-H35	1.0873

C17-N18-C20	126.1
H19-N18-C20	116.7
N18-C20=O21	122.6
N18-C20-C22	113.2
O21=C20-C22	124.1
C20-C22-H23	117.6
C20-C222-C24	120.4
H23-C22=C24	122.0
C22=C24-H25	115.9
C22=C24-C26	127.6
H25-C24-C26	116.5
C24-C26-C27	123.2
C24-C26-C28	118.4
C27-C26-C28	118.3
C26-C27-H29	120.1
C26-C27-C31	120.7
H29-C27-C31	119.2
C26-C28-H30	119.1
C26-C28-C32	121.0
H30-C28-C32	119.8
C27-C31-H33	119.8
C27-C31-C34	120.3
H33-C31-C34	119.8
C28-C32-C34	120.0
C28-C32-H36	119.9
C34-C32-H36	120.1
C31-C34-C32	119.6
C31-C34-H35	120.1
C32-C34-H35	120.2

C5-C6-C15-C17	-4.7
C5-N11-C13-O14	-178.0
C5-N11-C13-C17	0.8
H12-N11-C13-O14	2.1
H12-N11-C13-C17	179.1
C11-C13-C17-C15	-6.4
C11-C13-C17-N18	177.6
O14-C13-C17-C15	172.3
O14-C13-C17-N18	-3.7
C6-C15-C17-C13	8.5
C6-C15-C17-N18	-176.2
Cl16-C15-C17-C13	-168.8
Cl16-C15-C17-C18	6.5
C13-C17-N18-H19	21.9
C13-C17-N18-C20	-133.4
C15-C17-N18-H19	-153.6
C15-C17-N18-C20	51.1
C17-N18-C20-O21	-2.6
C17-N18-C20-C22	176.7
H19-N18-C20-O21	-157.0
H19-N18-C20-C22	22.3
N18-C20-C22-H23	1.9
N18-C20-C22-C24	178.5
O21-C20-C22-H23	-178.8
O21-C20-C22-C24	0.8
C20-C22-C24-H25	-0.0
C20-C22-C24-C26	-179.9
H23-C22-C24-H25	179.5
H23-C22-C24-C26	-0.4
C22-C24-C26-C27	-0.6
C22-C24-C26-C28	179.5
H25-C24-C26-C27	179.6
H25-C24-C26-C28	-0.4
C24-C26-C27-H29	-0.0

C24-C26-C27-C31	-180.0
C28-C26-C27-H29	179.9
C28-C26-C27-C31	0.0
C24-C26-C28-H30	-0.0
C24-C26-C28-C32	180.0
C27-C26-C28-H30	180.0
C27-C26-C28-C32	0.0
C26-C27-C31-H33	180.0
C26-C27-C31-C34	-0.0
H29-C27-C31-H33	0.0
H29-C27-C31-C34	-180.0
C26-C28-C32-C34	-0.0
C26-C28-C32-H36	180.0
H30-C28-C32-C34	-180.0
H30-C28-C32-C26	0.02
C27-C31-C34-C32	0.0
C27-C31-C34-H35	180.0
H33-C31-C34-C32	-180.0
H33-C31-C34-H35	0.0
C28-C32-C34-C31	0.0
C28-C32-C34-H35	-180.0
H36-C32-C34-C31	180.0
H36-C32-C34-H35	0.0

Table 2. Calculated wavenumbers (scaled), IR, Raman bands and assignments of (2*E*)-*N*-(4-chloro-2-oxo-1,2-dihydroquinolin-3-yl)-3-phenylprop-2-enamide

HF/6-31G(6D,7F)			B3LYP/6-31G(6D, 7F)			B3LYP/SDD			IR	Raman	Assignments[a]
$\upsilon(cm^{-1})$	IRI	R_A	$\upsilon(cm^{-1})$	IR_I	R_A	$\upsilon(cm^{-1})$	IR_I	R_A	$\upsilon(cm^{-1})$	$\upsilon(cm^{-1})$	-
3331	67.01	73.07	3452	46.86	114.37	3467	52.72	106.30	3377	-	υNH(100)
3329	71.94	72.52	3387	59.38	146.46	3419	57.32	192.73	3377	-	υNH(100)
2955	3.38	87.95	3113	3.73	89.37	3124	11.18	152.26	3168	3149	υCHI(98)
2930	8.46	395.69	3091	22.83	345.9	3109	31.81	314.02	-	-	υCHII(92)
2930	36.08	125.2	3020	26.74	342.7	3106	23.43	225.69	-	-	υCHI(100)
2923	36.79	64.07	3082	36.21	54.14	3095	42.25	44.72	-	-	υCHII(100)
2916	12.10	106.04	3078	9.50	119.9	3089	10.35	90.63	-	-	υCHI(99)
2914	5.94	55.44	3074	10.55	128.9	3084	10.61	108.49	3085	-	υCHII(93)
2909	23.57	50.95	3066	1.83	94.17	3074	4.04	60.51	-	-	υCHII(97)
2902	2.32	53.30	3062	5.52	69.26	3071	5.03	54.04	-	-	υCHI(97)
2901	0.48	131.06	3061	1.83	33.20	3069	8.34	42.39	-	-	υCHII(94)
2897	0.91	7.09	3060	10.34	11.76	3068	7.06	10.02	3062	3067	υCH(93)
2894	3.74	16.14	3052	0.21	30.06	3053	0.18	26.66	3029	3030	υCH(93)
1627	155.47	411.55	1719	60.45	68.01	1639	131.02	1544.09	1631	1648	υC=C(66), υCO(23)
1611	608.49	611.63	1690	545.4	42.13	1608	266.4	2489.9	1606	1601	υCC(21), υCO(12) υPhI(22)
1585	41.93	158.68	1630	229.4	3350.1	1595	50.54	415.84	-	-	υC=O(82), δNH(10)
1578	622.92	1432.6	1604	12.89	641.5	1593	33.09	36.07	-	-	υPhI(53), υC=C(12)

1570	62.33	48.77	1596	6.23	16.17	1587	3.57	1372.1	-	1585	υPhII(55), υPhI(20)
1561	3.32	388.43	1591	57.26	11.68	1577	436.51	2610.6	-	-	υC=O(57), υPhII(15)
1535	23.53	18.40	1571	13.73	100.9	1560	13.93	89.29	-	-	υPhII(66), δCHII(10)
1533	58.01	196.17	1560	0.93	877.2	1547	117.2	1518.9	-	-	υC=O(15), υPhI(32), υC=C(12)
1468	532.76	37.83	1487	94.06	0.42	1474	592.6	538.48	1490	-	δNH(59), υCN(31)
1451	15.93	14.89	1485	435.61	784.24	1469	2.52	62.77	-	-	δCHII(58), υPhII(40)
1449	22.83	3.45	1477	331.54	223.07	1464	166.56	25.22	-	-	υPhI(36), δNH(13)
1427	26.90	93.07	1461	33.43	149.55	1445	21.44	107.42	1449	1457	υPhII(49), υPhI(42)
1406	27.08	20.16	1440	23.91	92.96	1424	30.18	97.16	1402	1413	δCHII(15), υPhII(50)
1374	42.99	53.38	1392	10.14	103.39	1383	85.65	15.70	-	-	δNH(66), δCHI(14)
1312	108.65	33.24	1330	8.42	43.49	1347	7.85	291.46	-	-	υPhI(81)
1304	207.23	30.83	1324	229.29	8.43	1333	105.38	84.76	-	1334	υPhII(71)
1294	9.19	122.07	1322	144.96	167.87	1328	21.40	120.46	-	-	δCHI(90)
1267	83.07	4.99	1315	4.10	57.98	1323	209.18	9.57	-	1319	υCN(13), υCC(10)
1248	2.01	209.55	1304	48.94	57.96	1305	18.35	54.01	-	-	δCH(28), υCN(11), υCC(16)
1244	103.81	20.46	1273	22.22	2.94	1279	27.02	14.13	1285	1294	υCC(54), υPhII(10)
1211	38.85	73.15	1260	27.49	187.01	1268	41.80	146.68	-	-	υCC(30), υCN(27)
1197	25.82	12.73	1246	9.80	3.63	1246	10.62	16.03	1248	1253	υCN(19), δPhI(15), υPhI(14), δCHI(34)
1176	39.21	2.73	1223	22.73	74.61	1235	41.88	55.17	-	-	υPhI(21), δCHI(19),

											δNH(42)
1172	298.45	177.21	1193	54.14	427.22	1202	10.96	178.99	-	-	υCC(37), δCH(12), υPhII(18), δCHII(14)
1156	6.95	37.70	1183	136.69	204.18	1187	233.77	838.0	1196	1199	υCN(40), δCHII(25)
1149	8.79	83.35	1169	15.84	227.15	1177	15.40	207.1	-	1177	δCHII(73)
1125	128.9	97.11	1149	21.91	8.91	1163	20.84	6.80	-	-	δCHI (83)
1115	5.83	29.77	1148	0.81	23.68	1160	0.38	16.50	-	1150	δCHII(81)
1110	0.88	28.98	1128	280.2	692.44	1135	177.5	625.21	-	-	υCN(30), υCC(12), δCHI(12)
1081	8.80	18.49	1105	83.90	347.18	1103	34.31	164.78	1115	1114	υPhI(20), δCHI(48)
1040	5.08	0.75	1072	7.16	5.46	1068	9.10	1.01	1071	-	υPhII(29), δCHII(51)
1026	5.60	11.17	1032	5.38	54.37	1022	7.86	67.16	1030	1030	υPhI(67), δCHI(28)
1019	0.35	0.51	1018	0.35	39.64	1014	32.40	4.24	-	-	γC=C(24), τC=C(17), δCHII(45), τPhII(10)
1005	31.16	10.25	997	22.01	4.03	1009	2.61	32.45	-	-	υPhII(53), δPhII(13), δCHII(12)
996	1.30	31.42	979	13.86	19.20	1000	9.63	0.18	-	1000	γCHII(66), τPhII(11), γC=C(10)
992	1.04	0.06	977	15.96	105.21	992	0.01	0.39	-	-	γCHI(82), υPhI(11)
987	1.73	2.57	959	0.51	0.82	985	0.49	0.12	-	-	γCHII(91)
980	6.90	0.37	944	0.02	0.29	977	1.78	166.79	-	972	δPhII(63), υPhII(31)
962	1.20	91.38	933	1.97	19.44	960	27.48	5.73	968	-	δC=O(37), υCN(13),

											δNH(13)
947	27.22	3.36	931	0.01	0.25	957	4.07	0.58	-	944	γCHI(91)
938	2.83	5.52	919	13.48	3.27	929	0.02	0.42	937	-	γCHII(75), τPhII(12)
915	4.85	9.21	909	2.08	0.73	928	1.31	11.07	-	-	δPhI(24), δCN(15)
898	57.24	12.61	895	0.06	5.08	911	16.12	8.42	-	-	δPhI(39), δRing(12), υCCl(11), υCC(10)
892	6.98	22.85	849	24.01	14.29	882	23.67	23.23	-	-	γCH(62)
884	13.65	3.46	841	1.16	29.94	868	0.99	1.10	865	862	γCHI(76), τPhI(10)
849	1.23	3.96	831	0.41	5.10	848	1.68	0.34	-	848	γCHII(96)
826	12.23	11.14	824	9.40	20.42	839	9.73	8.36	841	-	υPhII(13), δCC(18), τPhII(18), γCHII(17)
795	27.36	5.75	820	1.03	6.69	810	15.66	30.55	-	-	υCCl(20), υPhI(14), τPhII(17), γCHII(14)
794	66.17	4.89	757	26.24	3.76	774	56.19	0.68	792	-	τPhII(28), γCHII(25), γCC(12)
777	218.55	0.93	750	45.75	1.82	771	176.35	0.86	-	-	γNH(16), τRing(15), γCHI(37), γCO(14)
768	63.56	0.95	740	69.34	1.90	766	15.81	2.73	-	765	τRing(25), γCO(14), γCN(11), γCHI(22)
751	1.59	1.65	718	0.20	1.39	740	8.10	2.50	758	-	τPhI(44), τRing(18)
730	12.44	2.94	717	9.58	3.12	728	7.09	12.43	-	-	τPhI(18), γNH(42), γCO(11)

704	9.04	3.93	693	19.48	1.67	704	15.76	1.68	-	-	γNH(31), δC=O(47), γCHII(14)
683	77.96	4.00	688	6.02	19.35	695	85.25	5.31	699	-	τPhII(25), δRing(11), γCHII(16)
677	7.22	3.23	665	29.24	11.58	686	33.69	2.05	-	-	τPhII(33), γCHII(16), γC=O(19)
666	11.25	4.77	638	76.96	20.21	668	14.14	13.92	675	666	γC=O(21), τPhII(11), γNH(44)
630	18.51	8.95	636	60.62	4.47	634	25.03	97.82	-	-	δPhI(31), γNH(11), τNH(10)
606	0.26	8.11	611	17.01	36.70	632	57.36	84.55	632	-	γNH(20), τNH(19), δPhI(16), τC=O(13)
603	18.68	2.50	609	10.10	38.34	611	0.41	16.06	-	619	δPhII(86)
592	4.50	3.73	604	3.35	1.56	598	3.21	9.83	-	-	δPhI(25), δCO(25), δCN(10)
562	103.39	29.05	565	18.43	5.68	576	3.51	24.42	-	-	υCCl(38), τPhI(26), τRing(20)
558	12.21	3.39	563	6.67	11.42	565	14.84	1.65	563	564	δPhII(50), τRing(22)
521	20.93	2.74	516	8.49	2.68	518	13.40	15.34	527	-	γCCl(18), τRing(24), τPhI(18), τPhII(11), γCN(17)
506	45.39	4.88	513	31.32	21.21	514	30.44	11.07	-	-	γC=O(29), δRing(14),

											δCC(13)
438	6.87	0.89	483	6.06	4.90	491	11.55	5.85	-	476	τPhII(26), γCC(32)
451	2.18	2.54	460	1.71	9.75	457	2.83	10.07	473	-	τPhI(25), τPhII(15), γCN(11)
441	10.43	17.83	443	2.04	38.84	444	3.80	52.51	-	-	τPhI(21), δRing(15)
410	20.92	2.15	417	21.34	1.22	418	20.84	1.84	-	-	δRing(24), δCC(28)
400	0.10	0.20	398	0.02	0.09	403	0.02	0.04	404	408	τPhII(85)
375	2.91	5.13	391	3.30	7.54	383	3.55	7.43	-	-	δCCl(27), δRing(24)
353	6.35	3.38	356	7.19	6.39	352	5.35	9.11	-	349	τPhI(28), γCCl(14)
310	13.24	3.45	323	6.04	1.69	314	7.66	2.00	-	-	δCO(22), δCN(11)
281	4.00	4.06	282	1.85	8.90	282	1.80	5.52	-	282	τPhII(38), τPhI(24)
275	2.24	3.73	269	4.32	101.2	271	3.78	4.28	-	-	τRing(36), τPhI(26)
255	14.0	3.88	266	3.45	0.46	265	10.91	8.72	-	262	τNH(11), τPhII(11), δCN(10)
237	3.63	1.79	245	2.20	1.39	242	1.86	1.06	-	-	δCC(39), δCO(17)
216	0.30	2.95	228	0.53	2.15	220	0.84	2.49	-	-	γCCl(50), τPhI(23)
186	4.84	0.87	188	3.33	2.85	185	3.64	2.79	-	-	δCCl(19), δC=O(10)
149	0.43	1.67	150	0.48	3.08	157	1.07	2.63	-	159	τC=C(27), τC=O(10)
128	0.22	3.32	138	0.18	2.51	144	0.34	1.90	-	-	τRing(24), γCCl(15), γNH(11), τPhII(10)
112	1.18	2.58	128	1.83	1.55	133	1.89	0.45	-	127	τNH(22), τC=C(19)
99	4.74	2.51	105	2.60	7.04	108	4.33	7.10	-	104	τRing(49), τNH(15)

89	2.56	1.77	93	0.64	3.37	93	0.93	3.64	-	-	τRing(17), τNH(13), τC=C(13)
70	1.83	2.22	77	0.67	4.35	80	1.12	5.22	-	-	τRing(23), τNH(34)
53	3.66	8.55	66	0.13	8.31	68	0.25	5.56	-	-	τNH(15), δCC(14), τRing(12)
28	1.86	4.52	29	1.05	6.06	30	0.51	8.46	-	-	τCC(41), τC=C(16)
20	2.14	1.94	27	0.05	10.64	27	1.02	6.41	-	-	τNH(17), δNH(25), δCN(14)
9	0.04	11.28	19	1.26	2.50	21	1.81	1.73	-	-	τC=O(46), γNH(17)

[a]υ-stretching; δ-in-plane deformation; γ-out-of-plane deformation;τ -torsion; Ph-phenyl ring; Ring-quinoline ring; potential energy distribution is given in brackets in the assignment column; IRI-IR intensity in KM/Mole; RA-Raman activity in $Å^4$/amu. PhII-mono-substituted phenyl ring; PhI-1,2-di-substituted phenyl ring; Ring-quinoline ring.

Table 3. Second-order perturbation theory analysis of Fock matrix in NBO basis corresponding to the intra molecular bonds of the title compound

Donor(i)	Type	ED/e	Acceptor(j)	Type	ED/e	E(2)[a]	E(j)-E(i)[b]	F(i,j)[c]
C1-C2	σ	1.97888	C1-C6	σ*	0.01443	1.91	1.21	0.043
-	σ	-	C2-C3	σ*	0.01632	1.53	1.22	0.039
-	σ	-	C6-C15	σ*	0.03418	4.84	1.15	0.067
C1-C6	σ	1.97012	C1-C2	σ*	0.01443	1.83	1.24	0.043
-	σ	-	C5-C6	σ*	0.03449	2.92	1.18	0.052
-	σ	-	C5-N11	σ*	0.02958	4.13	1.08	0.06
-	σ	-	C6-C15	σ*	0.03418	2.81	1.14	0.051
-	σ	-	C15-C17	σ*	0.03084	3.2	1.24	0.056
C1-C6	π	1.60294	C2-C3	π*	0.37051	20.34	0.28	0.068
-	π	-	C4-C5	π*	0.41199	24.62	0.27	0.073
-	π	-	C15-C17	π*	0.29246	21.12	0.27	0.069
C2-C3	σ	1.98046	C1-C2	σ*	0.01443	1.53	1.24	0.039
-	σ	-	C3-C4	σ*	0.01274	1.49	1.23	0.039
C2-C3	π	1.6147	C1-C6	π*	0.42392	24.66	0.27	0.074
-	π	-	C4-C5	π*	0.41199	21.1	0.26	0.067
C3-C4	σ	1.97824	C2-C3	σ*	0.01632	1.48	1.23	0.038
-	σ	-	C4-C5	σ*	0.02057	1.91	1.21	0.043
-	σ	-	C5-N11	σ*	0.02958	4.89	1.09	0.065
C4-C5	σ	1.97102	C3-C4	σ*	0.01274	1.79	1.25	0.042
-	σ	-	C5-C6	σ*	0.03449	3.17	1.2	0.055
-	σ	-	C5-N11	σ*	0.02958	0.98	1.09	0.029
-	σ	-	C6-C15	σ*	0.03418	4.03	1.16	0.061
-	σ	-	N11-C13	σ*	0.06847	4.44	1.09	0.063
C4-C5	π	1.62265	C1-C6	π*	0.42392	18.27	0.29	0.066
-	π	-	C2-C3	π*	0.37051	23.52	0.29	0.074
C5-C6	σ	1.9571	C1-C6	σ*	0.02158	2.62	1.21	0.05
-	σ	-	C4-C5	σ*	0.02057	2.99	1.21	0.054
-	σ	-	C6-C15	σ*	0.03418	2.46	1.15	0.048
-	σ	-	C15-Cl16	σ*	0.04032	4.88	0.77	0.055
C5-N11	σ	1.98455	C1-C6	σ*	0.02158	2.68	1.34	0.054
-	σ	-	C3-C4	σ*	0.01274	1.92	1.37	0.046

-	σ	-	C4-C5	σ*	0.02057	1.09	1.33	0.034
-	σ	-	C13-O14	σ*	0.00905	2.46	1.3	0.051
C6-C15	σ	1.97184	C1-C2	σ*	0.01443	2.55	1.25	0.051
-	σ	-	C1-C6	σ*	0.02158	2.99	1.21	0.054
-	σ	-	C4-C5	σ*	0.02057	3.56	1.21	0.059
-	σ	-	C5-C6	σ*	0.03449	1.83	1.19	0.042
-	σ	-	C15-C17	σ*	0.03084	2.81	1.25	0.053
-	σ	-	C17-N18	σ*	0.02833	5.51	1.1	0.069
N11-C13	σ	1.98567	C4-C5	σ*	0.02057	2.6	1.34	0.053
-	σ	-	C5-N11	σ*	0.02958	1.27	1.22	0.035
-	σ	-	C17-N18	σ*	0.02833	2.21	1.23	0.047
C13-O14	σ	1.98798	C5-N11	σ*	0.02958	3.19	1.38	0.06
-	σ	-	C13-C17	σ*	0.07091	1.14	1.39	0.036
-	σ	-	C15-C17	σ*	0.03084	2.14	1.54	0.052
C13-O14	π	1.97962	C13-O14	π*	0.39457	1.67	0.33	0.023
-	π	-	C15-C17	π*	0.29246	6.16	0.37	0.046
C13-C17	σ	1.95727	C15-Cl16	σ*	0.04032	6.78	0.75	0.064
-	σ	-	C15-C17	σ*	0.03084	2.92	1.23	0.054
-	σ	-	N18-C20	σ*	0.08318	3.84	1.07	0.058
C15-Cl16	σ	1.98008	C5-C6	σ*	0.03449	4.06	1.17	0.062
-	σ	-	C13-C17	σ*	0.07091	4.77	1.08	0.065
C15-C17	σ	1.97729	C1-C6	σ*	0.02158	3.6	1.28	0.061
-	σ	-	C6-C15	σ*	0.03418	2.6	1.22	0.05
-	σ	-	C13-O14	σ*	0.00905	1.92	1.24	0.044
-	σ	-	C13-C17	σ*	0.07091	1.73	1.16	0.04
-	σ	-	C17-N18	σ*	0.02833	2.49	1.16	0.048
C15-C17	π	1.79731	C1-C6	π*	0.42392	14.66	0.32	0.065
-	π	-	C13-O14	π*	0.39457	21.45	0.27	0.072
-	π	-	N18-C20	σ*	0.08318	1.57	0.68	0.03
C17-N18	σ	1.98161	C6-C15	σ*	0.03418	3.1	1.25	0.056
-	σ	-	N11-C13	σ*	0.06847	2.07	1.19	0.045
-	σ	-	C15-C17	σ*	0.03084	2.33	1.35	0.05
-	σ	-	C20-C22	σ*	0.05492	1.92	1.23	0.044
N18-H19	σ	1.9784	C15-C17	σ*	0.03084	4.79	1.2	0.068

-	σ	-	C20-O21	σ*	0.01687	3.7	1.15	0.058
N18-C20	σ	1.98135	C13-C17	σ*	0.07091	1.7	1.19	0.041
-	π	-	C15-C17	π*	0.29246	1.15	0.8	0.029
-	σ	-	C17-N18	σ*	0.02833	1.36	1.19	0.036
-	σ	-	C22-C24	σ*	0.01136	2.07	1.41	0.048
C20-O21	σ	1.99047	C20-C22	σ*	0.05492	1.22	1.43	0.038
-	π	-	C22-C24	π*	0.11155	4.15	0.39	0.037
C20-C22	σ	1.96942	C17-N18	σ*	0.02833	5.88	1.05	0.07
-	σ	-	C22-C24	σ*	0.01136	2.02	1.27	0.045
-	σ	-	C24-C26	σ*	0.0241	5.49	1.13	0.07
C22-H23	σ	1.97812	C20-O21	σ*	0.01687	4.37	1.03	0.06
-	σ	-	C22-C24	σ*	0.01136	1.11	1.14	0.032
C22-C24	σ	1.97924	N18-C20	σ*	0.08318	2.51	1.11	0.048
-	σ	-	C20-C22	σ*	0.05492	1.57	1.16	0.038
-	σ	-	C24-C26	σ*	0.0241	2.03	1.2	0.044
-	σ	-	C26-C28	σ*	0.02323	2.87	1.25	0.054
C22-C24	π	1.84587	C20-O21	π*	0.31371	23.25	0.27	0.073
-	σ	-	C26-C28	σ*	0.37582	12.31	0.3	0.058
C24-C26	σ	1.97271	C20-C22	σ*	0.05492	3.44	1.09	0.055
-	σ	-	C22-C24	σ*	0.01136	2.31	1.27	0.049
-	σ	-	C26-C27	σ*	0.02776	1.85	1.18	0.042
-	σ	-	C26-C28	σ*	0.02323	1.69	1.18	0.04
-	σ	-	C27-C31	σ*	0.01414	2.9	1.21	0.053
-	σ	-	C28-C32	σ*	0.01449	3.24	1.2	0.056
C26-C27	σ	1.97406	C22-C26	σ*	0.0241	1.97	1.15	0.042
-	σ	-	C26-C28	σ*	0.02323	2.46	1.21	0.049
-	σ	-	C27-C31	σ*	0.01414	1.95	1.23	0.044
C26-C28	σ	1.97327	C22-C24	σ*	0.01136	3.12	1.29	0.057
-	σ	-	C24-C26	σ*	0.0241	1.78	1.15	0.04
-	σ	-	C26-C27	σ*	0.02776	2.45	1.2	0.048
-	σ	-	C28-C32	σ*	0.01449	1.8	1.22	0.042
C26-C28	π	1.6177	C22-C24	π*	0.11155	18.48	0.28	0.07
-	π	-	C27-C31	π*	0.29814	20.04	0.28	0.068
-	π	-	C32-C32	π*	0.32393	20.95	0.28	0.069

C27-C31	σ	1.98005	C24-C26	σ*	0.0241	4.52	1.16	0.065
-	σ	-	C26-C27	σ*	0.02776	2.01	1.21	0.04
-	σ	-	C31-C34	σ*	0.01643	1.61	1.22	0.04
C27-C31	π	1.67514	C26-C28	π*	0.37582	20.42	0.28	0.069
-	π	-	C32-C34	π*	0.32393	21.15	0.28	0.069
C28-C32	σ	1.98001	C24-C26	σ*	0.0241	4.12	1.62	0.062
-	σ	-	C26-C28	σ*	0.02323	1.81	1.21	0.042
-	σ	-	C32-C34	σ*	0.32393	1.63	1.23	0.04
C31-H33	σ	1.97739	C26-C27	σ*	0.02776	5.38	1.04	0.067
C31-C34	σ	1.98106	C27-C31	σ*	0.01414	1.62	1.23	0.04
-	σ	-	C32-C34	σ*	0.01623	1.5	1.22	0.038
C32-C34	σ	1.9813	C28-C32	σ*	0.01449	1.62	1.23	0.04
-	σ	-	C31-C34	σ*	0.01643	1.49	1.22	0.038
C32-C34	π	1.65247	C26-C28	π*	0.37582	21.73	0.28	0.07
-	π	-	C27-C31	π*	0.29814	20.11	0.28	0.068
LPN11	σ	1.62269	C4-C5	π*	0.41199	38.54	0.29	0.096
-	σ	-	C13-O14	π*	0.39457	63.78	0.26	0.115
LPO14	σ	1.97573	N11-C13	σ*	0.06847	1.87	1.07	0.041
-	σ	-	C13-C17	σ*	0.07091	3.1	1.08	0.052
LPO14	π	1.87789	C5-N11	σ*	0.02958	0.55	0.64	0.017
-	π	-	N11-C13	σ*	0.06847	21.92	0.64	0.108
-	π	-	C13-C17	σ*	0.07091	16.25	0.65	0.093
LPCl16	σ	1.98948	C6-C15	σ*	0.03418	2.31	1.38	0.051
-	σ	-	C15-C17	σ*	0.03084	2.1	1.47	0.05
LPCl16	π	1.97019	C6-C15	σ*	0.03418	3.46	0.77	0.046
-	π	-	C15-C17	σ*	0.03084	4.34	0.86	0.055
-	π	-	C15-C17	π*	0.29246	12.68	0.32	0.06
LPN18	σ	1.68465	C13-C17	σ*	0.07091	3.49	0.66	0.046
-	σ	-	C15-C17	σ*	0.03084	1.5	0.82	0.034
-	σ	-	C15-C17	π*	0.29246	26.61	0.28	0.077
-	σ	-	C20-O21	σ*	0.01687	1.18	0.77	0.029
-	σ	-	C20-O21	π*	0.31371	49.35	0.27	0.103
LPO21	σ	1.9755	N18-C20	σ*	0.08318	1.74	1.05	0.039
-	σ	-	C20-C22	σ*	0.05492	3.28	1.1	0.054

LPO21	π	1.8785	N18-C20	σ*	0.08318	25.5	0.63	0.114
-	π	-	C20-C22	σ*	0.05492	16.1	0.67	0.094

---

[a]E(2) means energy of hyperconjugative interactions (stabilization energy).

[b]Energy difference between donor and acceptor i and j NBO orbitals.

[c]F(i,j) is the Fock matrix element between i and j NBO orbitals.

Table 4. NBO results showing the formation of Lewis and non-Lewis orbitals

Bond(A-B)	ED/energy[a]	EDA%	EDB%	NBO	s%	p%
σC1-C2	1.97888	50.48	49.52	0.7105($sp^{1.79}$)C+	35.90	64.10
-	-0.70661	-	-	0.7037($sp^{1.79}$)C	35.78	64.22
σC1-C6	1.97012	48.08	51.92	0.6934($sp^{1.88}$)C+	34.73	65.27
-	-0.70038	-	-	0.7205($sp^{1.87}$)C	34.86	65.14
πC1-C6	1.60294	46.23	53.77	0.6800($sp^{1.00}$)C+	0.00	100.0
-	-0.26427	-	-	0.7333($sp^{1.00}$)C	0.00	100.0
σC2-C3	1.98046	49.79	50.21	0.7056($sp^{1.87}$)C+	34.85	65.15
-	-0.69650	-	-	0.7086($sp^{1.83}$)C	35.34	64.66
πC2-C3	1.61470	51.35	48.65	0.7166($sp^{1.00}$)C+	0.00	100.0
-	-0.26041	-	-	0.6975($sp^{1.00}$)C	0.00	100.0
σC3-C4	1.97824	49.34	50.66	0.7024($sp^{1.82}$)C+	35.45	64.55
-	-0.71141	-	-	0.7118($sp^{1.76}$)C	36.24	63.76
σC4-C5	1.97102	48.61	51.39	0.6972($sp^{1.88}$)C+	34.74	65.26
-	-0.71786	-	-	0.7169($sp^{1.74}$)C	36.48	63.52
πC4-C5	1.62265	52.03	47.97	0.7213($sp^{1.00}$)C +	0.00	100.0
-	-0.27729	-	-	0.6926($sp^{1.00}$)C	0.00	100.0
σC5-C6	1.95710	49.76	50.24	0.7054($sp^{1.78}$)C +	35.96	64.04
-	-0.70946	-	-	0.7088($sp^{2.06}$)C	32.66	67.34
σC5-N11	1.98455	37.54	62.46	0.6127 ($sp^{2.65}$)C +	27.42	72.58
-	-0.83825	-	-	0.7903($sp^{1.63}$)N	37.96	62.04
σC6-C15	1.97184	50.05	49.95	0.7075($sp^{2.08}$)C +	32.43	67.57
-	-0.71285	-	-	0.7068($sp^{1.59}$)C	38.54	61.46
σN11-C13	1.98567	63.64	36.36	0.7978($sp^{1.82}$)N +	35.47	64.53
-	-0.84394	-	-	0.6030($sp^{2.23}$)C	30.95	69.05
σC13-O14	1.98798	35.10	64.90	0.5925($sp^{2.05}$)C +	32.83	67.17
-	-1.00514	-	-	0.8056($sp^{1.90}$)O	34.54	65.46
πC13-O14	1.97962	29.12	70.88	0.5396($sp^{99.99}$)C +	0.02	99.98
-	-0.37008	-	-	0.8419($sp^{99.99}$)O	0.03	99.97
σC13-C17	1.95727	48.39	51.61	0.6956($sp^{1.76}$)C +	36.26	63.74
-	-0.68837	-	-	0.7184($sp^{2.22}$)C	31.09	68.91
σC15-Cl16	1.98008	43.62	56.38	0.6605($sp^{3.67}$)C +	21.41	78.59
-	-0.69515	-	-	0.7508($sp^{5.44}$)Cl	15.52	84.48

σC15-C17	1.97729	49.82	50.18	0.7058($sp^{1.50}$)C +	40.07	59.93
-	-0.77463	-	-	0.7084($sp^{1.53}$)C	39.52	60.48
πC15-C17	1.79731	50.31	49.69	0.7093($sp^{1.00}$)C +	0.01	99.99
-	-0.30779	-	-	0.7049($sp^{99.99}$)C	0.02	99.98
σC17-N18	1.98161	38.89	61.11	0.6236($sp^{2.41}$)C +	29.29	70.71
-	-0.81081	-	-	0.7817($sp^{1.81}$)N	35.54	64.46
σN18-C20	1.98135	64.00	36.00	0.8000($sp^{1.83}$)N +	35.35	64.65
-	-0.80125	-	-	0.6000($sp^{2.32}$)C	30.08	69.92
σC20-O21	1.99047	34.44	65.56	0.5868($sp^{2.04}$)C +	32.85	67.15
-	-1.00730	-	-	0.8097($sp^{1.77}$)O	36.05	63.95
πC20-O21	1.97678	30.92	69.08	0.5561($sp^{99.99}$)C +	0.18	99.82
-	-0.35859	-	-	0.8311($sp^{99.99}$)O	0.13	99.87
σC20-C22	1.96942	49.18	50.82	0.7013($sp^{1.70}$)C +	37.00	63.00
-	-0.66370	-	-	0.7129($sp^{2.13}$)C	31.95	68.05
σC22-C24	1.97924	50.02	49.98	0.7072($sp^{1.61}$)C +	38.37	61.63
-	-0.73205	-	-	0.7070($sp^{1.68}$)C	37.27	62.73
πC22-C24	1.84587	54.44	45.56	0.7379($sp^{1.00}$)C +	0.00	100.0
-	-0.27435	-	-	0.6750($sp^{1.00}$)C	0.00	100.0
σC24-C26	1.97271	49.46	50.54	0.7033($sp^{1.84}$)C +	35.17	64.83
-	-0.66244	-	-	0.7109($sp^{2.09}$)C	32.39	67.61
σC26-C27	1.97406	50.63	49.37	0.7116($sp^{1.93}$)C +	34.15	65.85
-	-0.68602	-	-	0.7026($sp^{1.81}$)C	35.56	64.44
σC26-C28	1.97327	50.79	49.21	0.7127($sp^{1.99}$)C +	33.45	66.55
-	-0.68474	-	-	0.7015($sp^{1.80}$)C	35.75	64.25
πC26-C28	1.61770	51.63	48.37	0.7186($sp^{1.00}$)C +	0.00	100.0
-	-0.24925	-	-	0.6955($sp^{1.00}$)C	0.00	100.0
σC27-C31	1.98005	50.33	49.67	0.7095($sp^{1.80}$)C +	35.66	64.34
-	-0.69523	-	-	0.7047($sp^{1.80}$)C	35.73	64.27
πC27-C31	1.67514	49.55	50.45	0.7039 ($sp^{1.00}$)C +	0.00	100.0
-	-0.25567	-	-	0.7103($sp^{1.00}$)C	0.00	100.0
σC28-C38	1.98001	50.23	49.77	0.7087($sp^{1.82}$)C+	35.42	64.58
-	-0.69284	-	-	0.7055($sp^{1.81}$)C	35.59	64.41
σC31-C34	1.98106	50.06	49.94	0.7075($sp^{1.84}$)C+	35.24	64.76
-	-0.68950	-	-	0.7067($sp^{1.83}$)C	35.29	64.71

σC32-C34	1.98130	50.04	49.96	0.7074($sp^{1.83}$)C+	35.30	64.70
-	-0.69131	-	-	0.7068($sp^{1.82}$)C	35.43	64.57
πC32-C34	1.65247	50.37	49.63	0.7097($sp^{1.00}$)C+	0.00	100.0
-	-0.25328	-	-	0.7045($sp^{1.00}$)C	0.00	100.0
n1N11	1.62269	-	-	$sp^{1.00}$	0.00	100.0
-	-0.29286	-	-	-	-	-
n1O14	1.97573	-	-	$sp^{0.53}$	65.45	34.55
-	-0.69816	-	-	-	-	-
n2O14	1.87789	-	-	$sp^{99.99}$	0.01	99.99
-	-0.26770	-	-	-	-	-
n1Cl16	1.98948	-	-	$sp^{0.19}$	84.08	15.92
-	-0.93461	-	-	-	-	-
n2Cl16	1.97019	-	-	$sp^{99.99}$	0.30	99.70
-	-0.32163	-	-	-	-	-
n3Cl16	1.92000	-	-	$sp^{99.99}$	0.10	99.90
-	-0.31704	-	-	-	-	-
n1N18	1.68465	-	-	$sp^{40.77}$	2.39	97.61
-	-0.27708	-	-	-	-	-
n1O21	1.97550	-	-	$sp^{0.57}$	63.83	36.17
-	-0.67333	-	-	-	-	-
n2O21	1.87847	-	-	$sp^{99.99}$	0.02	99.98
-	-0.24881	-	-	-	-	-

[a]ED/energy in a.u.

Table 5. The charge distribution calculated by the Mulliken and natural bond orbital (NBO) methods

Atoms	Atomic charges(Mulliken)	Natural charges
C 1	-0.345525	-0.17545
C 2	-0.238086	-0.21833
C 3	-0.199086	-0.18774
C 4	-0.358573	-0.24225
C 5	0.249502	0.21526
C 6	0.395314	-0.11596
H 7	0.253772	0.23741
H 8	0.228895	0.22651
H 9	0.228456	0.22609
H 10	0.227403	0.22182
N 11	-0.408546	-0.61614
H 12	0.338060	0.43605
C13	0.002780	0.66961
O 14	-0.310708	-0.67035
C 15	-0.308734	0.04137
Cl 16	-0.003157	-0.01493
C 17	0.379675	0.09414
N18	-0.485967	-0.66435
H 19	0.338649	0.43870
C 20	0.221051	0.68427
O 21	-0.266928	-0.63171
C22	-0.368046	-0.29546
H 23	0.210216	0.20414
C24	-0.209379	-0.13039
H25	0.259279	0.23584
C26	0.465782	-0.07121
C27	-0.359596	-0.18996
C28	-0.379763	-0.18550
H29	0.220102	0.21314

H30	0.230879	0.22077
C31	-0.229151	-0.20733
C32	-0.225257	-0.21008
H33	0.221822	0.22156
C34	-0.223287	-0.20293
H35	0.224931	0.22118
H36	0.223221	0.22221

Table 6. Calculated Mulliken charges of (2*E*)-*N*-(4-chloro-2-oxo-1,2-dihydroquinolin-3-yl)-3-phenylprop-2-enamide

Atom	HF/6-31G	B3LYP/631g(6D,7F)	B3LYP/SDD
C1	-0.163705	-0.211917	-0.344756
C2	-0.217147	-0.130019	-0.238287
C3	-0.177899	-0.134010	-0.199404
C4	-0.193854	-0.175899	-0.359437
C5	0.456201	0.367035	0.249991
C6	-0.084068	0.118661	0.394645
H7	0.256455	0.166311	0.254905
H8	0.215136	0.139361	0.228931
H9	0.217897	0.138627	0.226700
H10	0.222213	0.133986	0.225575
N11	-1.093868	-0.774533	-0.408703
H12	0.407401	0.339648	0.336836
C13	0.821171	0.610691	0.002627
O14	-0.609070	-0.540193	-0.310699
C15	-0.205201	-0.113494	-0.309263
Cl16	0.223213	0.053239	0.003166
C17	0.234013	0.236515	0.379525
N18	-0.975891	-0.717541	-0.483719
H19	0.405865	0.356844	0.340841
C20	0.787030	0.601297	0.219798
O21	-0.622511	-0.505872	-0.272513
C22	-0.271346	-0.213347	-0.365540
H23	0.199169	0.139117	0.213864
C24	-0.103524	-0.155752	-0.212156
H25	0.251119	0.164620	0.256019
C26	-0.052777	0.169616	0.466976
C27	-0.173467	-0.171890	-0.358091
C28	-0.207271	-0.187155	-0.382172
H29	0.210824	0.138031	0.223246

H30	0.218755	0.134672	0.226518
C31	-0.206186	-0.131264	-0.228202
C32	-0.203512	-0.131344	-0.226061
H33	0.206399	0.142139	0.226673
C34	-0.186392	-0.124182	-0.223017
H35	0.206939	0.136823	0.225920
H36	0.207891	0.131178	0.219263

Table7. Experimental and calculated ^{1}H NMR parameters (with respect to TMS).

Protons	σ_{TMS}	B3LYP/SDD	$\delta_{calc} = \sigma_{TMS} - \sigma_{calc}$	Exp.(δ_{ppm})
7H	32.7711	24.3451	8.462	7.51
8H	-	24.9830	7.7881	7.30
9H	-	24.9113	7.8598	7.40
10H	-	25.5397	7.2314	7.20
12H	-	25.0065	7.7646	7.30
19H	-	24.9365	7.8346	7.40
23H	-	26.0422	6.7289	6.70
25H	-	25.2490	7.5221	5.90
29H	-	24.5444	8.2267	7.51
30H	-	24.9566	7.8145	7.80
33H	-	24.8819	7.8892	7.4 0
35H	-	24.8266	7.9445	7.51
36H	-	24.8524	7.9187	7.80

Graphical abstract

Title of the paper: Vibrational spectroscopic and molecular docking study of (2*E*)-*N*-(4-chloro-2-oxo-1,2-dihydroquinolin-3-yl)-3-phenylprop-2-enamide

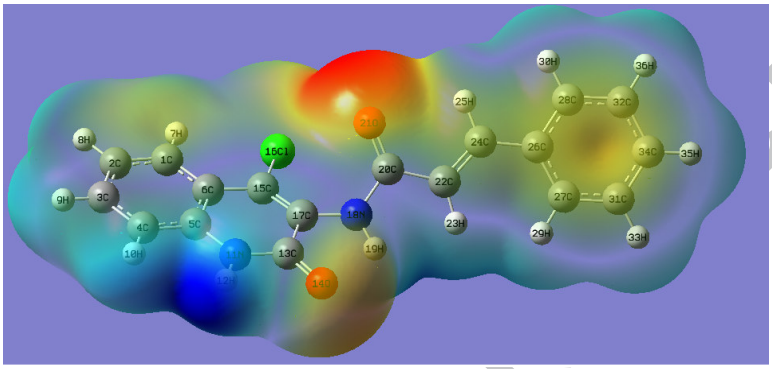

Highlights

* IR, Raman spectra and NBO analysis were reported.

* The wavenumbers are calculated theoretically using Gaussian09 software.

* The geometrical parameters are in agreement with that of similar derivatives.

* Molecular docking is reported.